RECORDS ADMINISTRATION
R0139042

DP-1565

CORRELATION OF NUCLEAR CRITICALITY SAFETY COMPUTER CODES WITH PLUTONIUM BENCHMARK EXPERIMENTS AND DERIVATION OF SUBCRITICAL LIMITS

H. K. CLARK

TIS FILE
RECORD C

E. I. du Pont de Nemours & Co.
Savannah River Laboratory
Aiken, SC 29808

PREPARED FOR THE U. S. DEPARTMENT OF ENERGY UNDER CONTRACT DE-AC09-76SR00001

DISCLAIMER

This report was prepared by E. I. du Pont de Nemours and Company (Du Pont) for the United States Department of Energy under Contract DE-AC09-76SR00001 and is an account of work performed under that Contract. Neither the United States, the United States Department of Energy nor Du Pont, nor any of their employees, makes any warranty, express or implied, or assumes any legal liability or responsibility for the accuracy, completeness, or usefulness of any information, apparatus, product, or process disclosed herein, or represents that its use will not infringe privately owned rights. Reference herein to any specific commerical product, process, or service by trade name, mark, manufacturer, or otherwise does not necessarily constitute or imply endorsement, recommendation, or favoring of same by Du Pont or by the United States Government or any agency thereof. The views and opinions of authors expressed herein do not necessarily state or reflect those of the United States Government or any agency thereof.

Printed in the United States of America

Available from

National Technical Information Service
U. S. Department of Commerce
5285 Port Royal Road
Springfield, Virginia 22161

Price: Printed Copy A04; Microfiche A01

726402

DP-1565
UC Category: 34C

CORRELATION OF NUCLEAR CRITICALITY SAFETY COMPUTER CODES WITH PLUTONIUM BENCHMARK EXPERIMENTS AND DERIVATION OF SUBCRITICAL LIMITS

H. K. Clark

Approved by:

M. M. Anderson, Jr., Research Manager
Nuclear Physics Division

Publication date: October 1981

Issued by E. I. du Pont de Nemours & Co.
Savannah River Laboratory
Aiken, SC 29808

PREPARED FOR THE U. S. DEPARTMENT OF ENERGY UNDER CONTRACT DE-AC09-76SR00001

ABSTRACT

A compilation of benchmark critical experiments was made for essentially one-dimensional systems containing plutonium. The systems consist of spheres, series of experiments with cylinders and cuboids that permit extrapolation to infinite cylinders and slabs, and large cylinders for which separability of the neutron flux into a product of spatial components is a good approximation. Data from the experiments were placed in a form readily usable as computer code input. Aqueous solutions of $Pu(NO_3)_4$ are treated as solutions of PuO_2 in nitric acid. The apparent molal volume of PuO_2 as a function of plutonium concentration was derived from analyses of solution density data and was incorporated in the Savannah River Laboratory computer codes along with density tables for nitric acid.

The biases of three methods of calculation were established by correlation with the benchmark experiments. The oldest method involves two-group diffusion theory and has been used extensively at the Savannah River Laboratory. The other two involve S_n transport theory with, in one method, Hansen-Roach cross sections and, in the other, cross sections derived from ENDF/B-IV. Subcritical limits were calculated by all three methods. Significant differences were found among the results and between the results and limits currently in the American National Standard for Nuclear Criticality Safety in Operations with Fissionable Materials Outside Reactor (ANSI N16.1), which were calculated by yet another method, despite the normalization of all four methods to the same experimental data. The differences were studied, and a set of subcritical limits was proposed to supplement and in some cases to replace those in the ANSI Standard, which is currently being reviewed.

CONTENTS

Introduction 5

Summary 6

Computational Methods 6

MGBS, TGAN, and KEFF 7

HRXN 8

GLASS 11

ANISN 15

SPBL 16

KENO 16

Experimental Data 17

$Pu(NO_3)_4$ Solution 17

PuO_2 - Plastic Compacts 25

Pu Metal 29

Correlations 29

$Pu(NO_3)_4$ Solution Spheres 32

$Pu(NO_3)_4$ Solution Slabs 42

$Pu(NO_3)_4$ Solution Cylinders 42

PuO_2 Compacts 45

Plutonium Metal 51

Subcritical Limits 52

References 61

Appendix A A-1

Appendix B B-1

CORRELATION OF NUCLEAR CRITICALITY SAFETY COMPUTER CODES WITH PLUTONIUM BENCHMARK EXPERIMENTS AND DERIVATION OF SUBCRITICAL LIMITS

INTRODUCTION

A number of computer codes are used at the Savannah River Laboratory (SRL) for nuclear criticality safety evaluations. The earlier codes were written here (originally for an IBM 650), principally for such evaluations. As computing machinery has improved (currently IBM System 360 Model 195 and System 370 Model 158), these codes have been adapted to the new machines,[1] and other codes have been added. The S_n computer code ANISN[2] and the Monte Carlo code KENO[3] have been obtained from Oak Ridge National Laboratory (ORNL). The development of the JOSHUA System[4] at SRL, with its modular concept, has permitted the linking of codes and facilitated the handling of data and the preparation of input. A driver subsystem KOKO has been written to perform such tasks[5]. A component of the JOSHUA System is the Generalized Lattice Analysis Subsystem (GLASS), which is intended for Savannah River Plant (SRP) reactor computations but which has been adapted to criticality safety evaluations. Access to ENDF/B-IV cross sections is provided by GLASS so that these cross sections may be used in addition to or instead of Hansen-Roach cross sections[6] commonly used with ANISN or KENO. It is expected that the development of computational methods, consisting of computer codes and associated numerical parameters such as cross sections, will continue as codes are improved or revised, as better cross sections become available, and perhaps as errors are discovered and corrected in existing methods; however, the methods presently in use are fairly well standardized, and changes are not expected in the immediate future.

A sine qua non in criticality safety evaluations is the correlation of any computational method with pertinent data obtained in critical experiments to indicate the bias to be expected from the method. So as not to build up a huge investment in correlations for a method that may become obsolete (e.g. by the incorporation of improved cross sections), the tendency is to correlate on an ad hoc basis. With the current fairly stable state of the methods, however, more extensive correlations appear warranted. Moreover, except for KENO, the codes are one-dimensional and quite fast on the present computer; therefore, if there are changes, the repetition of correlations should not prove inordinately expensive, particularly since data for one-dimensional systems, or data capable of being extrapolated thereto, are somewhat limited. Incidentally, where the method comprises a reasonably exact solution of the transport equation, the bias established with a particular set of cross sections should be applicable to any other reasonably exact solution (e.g. Monte Carlo) with the same set. Therefore,

there is special interest in data for one-dimensional systems and, at SRL and SRP particularly, for plutonium systems. The conversion of these data into computer code input generally requires some judgments and assumptions. It is desirable to preserve an exact record of the input so that subsequent correlations are facilitated and so that any differences can clearly be ascribed to changes in the computational method rather than to a reinterpretation of the data.

SUMMARY

This report contains a compilation of data obtained in critical experiments with plutonium systems, for the most part with one-dimensional systems. The data have been put in a form directly usable as computer code input.

The report describes three methods of calculation commonly used at SRL and gives biases of the methods established by correlations with the data. The biases are expressed as the critical value of k_{eff} and in some cases are appreciable. For aqueous solutions in which the plutonium contains about 5% ^{240}Pu or less, k_{eff} differs from unity by as much as 0.04, depending on concentration. On the other hand, for plutonium metal, k_{eff} differs by less than 0.01 from unity. Despite differences in sophistication in the methods, none is a clear choice on the basis of bias; approximately the same range is shown by all, although the variation with composition variables differs.

Finally, the biases are used as a basis for computing subcritical limits for simple systems by all three methods. The limits are compared with each other and with limits now in the American National Standard for Nuclear Criticality Safety in Operations with Fissionable Materials Outside Reactors (ANSI N16.1), currently under review, and revised and supplementary limits are proposed. Reduced limits for solutions of plutonium nitrate in which the plutonium is 100% ^{239}Pu are proposed for mass, cylinder diameter, slab thickness, and volume. It is proposed that the concentration limit be increased to its former value. Additional limits for solutions and PuO_2-H_2O slurries are proposed that take credit for ^{240}Pu. Limits for metal are confirmed, and limits for PuO_2 are proposed.

COMPUTATIONAL METHODS

As defined in the American National Standard for Validation of Calculational Methods for Nuclear Criticality Safety N16.9-1975, a calculational method is "the mathematical equations, approximations, assumptions, associated numerical parameters (e.g., cross

sections), and calculational procedures which yield the calculated results." Therefore, in the present work, a method is a particular combination of computer codes used in a particular manner with a particular set of cross sections.

Exact descriptions of the computer code input are contained in internal memoranda that will be made available to anyone obtaining the JOSHUA System[4] and the computer codes. They are not otherwise of much interest, but descriptions of how the codes are used and the operations they perform are of general interest. Descriptions of the three computational methods used in this study will be confined to the latter. The three methods are a two-group diffusion theory calculation with a rather old library of cross sections as implemented by MGBS-TGAN and two 16-group S_n transport theory calculations as carried out by ANISN with, in one method, Hansen-Roach cross sections as processed by HRXN and in the other, largely ENDF/B-IV cross sections as processed by GLASS. The S_n transport calculations were supplemented in some cases by Monte Carlo, with the same cross sections, as carried out by KENO. Descriptions of the codes follow.

MGBS, TGAN, and KEFF

The operations performed by the codes MGBS, TGAN, and KEFF have already been described[1]. MGBS performs a 12-group B_0 calculation to determine buckling and two-group diffusion theory parameters for use in the analytical code TGAN. KEFF uses TGAN results to calculate k_{eff} as $k/(1 + M^2B_g{}^2)$. Together, these codes form a computational method since MGBS contains its library of cross sections. The principal changes in these codes in the intervening years have been to convert them into JOSHUA modules, to provide for submission of input by way of JOSHUA records prepared at a terminal, and to link them by a driver module KOKO so that output from one forms part of the input for another. Modules executed by KOKO were also written to prepare input for special types of problems.

In the thermal group of MGBS, the cross sections are taken from Amster's compendium.[7] The thermal spectrum is characterized by the ratios $^{235}U/H$, $^{239}Pu/H$ and 1/v barns/H and by temperature. Cross sections at $4 \leq H/^{239}Pu < 100$ were obtained by extrapolating Amster's results.* It is expected that the accuracy of the

---

* Until recently, the fission cross section of ^{241}Pu was not extrapolated into this range; it was zero. It has now been extrapolated, the same constant value of α (σ_c/σ_f) is assumed as for $H/^{239}Pu \geq 100$. Although not pertinent here, constant values of cross sections for $2 < H/^{235}U < 50$ have now been replaced by extrapolation of Amster's results. These changes eliminate small step function changes when the $H/^{235}U$ or $H/^{239}Pu$ boundaries are crossed.

extrapolation decreases with its extent, but exact values of thermal cross sections are not very important in these hard spectra.

The fast group parameters generated by MGBS for fissionable materials are weighted by the spectrum obtained at critical buckling (without adjustment for any bias determined by correlation with experiment). Those for reflectors are weighted by the spectrum obtained at zero buckling. The latter spectrum is also used for weighting the cross sections for the materials in vessel walls. With the two-group parameters and specified dimensions, TGAN can perform two searches: a critical transverse buckling search and a critical zone width search. The buckling search may be requested for slab, cylinder, or sphere. For the sphere, it results in a fictitious buckling component which is subtracted from the critical (material) buckling of each material and which is adjusted until criticality is achieved with the specified dimensions. Just as for the slab or cylinder, the geometric buckling of the core is then

$$B_g^2 = B_c^2 - B_r^2$$

where B_c^2 is the critical (material) buckling determined by MGBS and B_r^2 is the critical transverse buckling. The value of k_{eff} is computed by KEFF simply as

$$k_{eff} = \frac{1 + M^2 B_c^2}{1 + M^2 B_g^2}$$

where the migration area is also determined by MGBS. Clearly, if calculation and experiment agree for a sphere, $k_{eff} = 1$ since the fictitious transverse buckling will be zero. In the dimension search, k_{eff} is specified (it defaults to unity); the corresponding transverse buckling is computed from core material cross sections; and a specified zone width (e.g. the core radius) is adjusted until criticality is achieved with this buckling.

HRXN

A separate module HRXN has been written at SRL to prepare macroscopic Hansen-Roach cross sections[6] as input to either ANISN or KENO. The microscopic cross sections are essentially those furnished with KENO-IV[3] and include the original Hansen-Roach sets together with sets generated subsequently at ORNL and LASL. Some changes have been made at SRL. All thermal cross sections were examined for conformity with BNL-325 and with the Chart of Nuclides. Modifications were made where indicated. Some were found not to be averages over a Maxwellian spectrum and were corrected. The cross sections have been placed in JOSHUA records

within a permanent data base. Resonance shielded cross sections are tabulated in these records for 20 values of potential scattering: 20, 40, 60, 100, 200, . . ., 10^6 barns per atom of nuclide. Interpolation and extrapolation within HRXN are 3-point Lagrange in terms of the logarithm of the potential scattering except at the upper end where extrapolation is linear and the extrapolated value is not allowed to exceed the value at infinite dilution. At the lower end, the extrapolated value is not allowed to rise once the minimum value for potential scattering less than 20 has been reached. For some nuclides, notably plutonium-238 and plutonium-240, graphical interpolation and extrapolation were required to obtain the cross sections at the selected values of potential scattering. Potential scattering cross sections and atomic weights (carbon-12 = 12.00000) are contained in a JOSHUA record within a permanent data base. HRXN automatically computes the potential scattering per nuclide and the corresponding resonance shielded cross sections. Wherever hydrogen was involved in experiments with which correlations were made, the set produced with $\chi(E)$ weighting (Tables XIX and XX of Reference 6) was selected.

A wide variety of ways is provided for submitting composition data, including, if desired, atom densities. The way adopted for aqueous solutions of $Pu(NO_3)_4$ was to treat them as solutions of PuO_2 in nitric acid. Nitric acid density tables derived from International Critical Tables are incorporated in HRXN for acid molarites ranging from 0 to 16 and temperatures from 15° to 30°C. Apparent molal volumes of PuO_2 derived from an analysis of density data[8-10] are also incorporated. Analysis of $Pu(NO_3)_4$ density and composition data in this manner shows wide scatter in the apparent molal volume, especially at low concentration, too much to permit detection of a conceivable dependence on free nitric acid molarity. Part of the scatter is no doubt due to inconsistency of the data. Nitrate ion concentration often does not agree well with that which should be associated with reported H^+ and Pu^{++++} concentrations. The molal volumes adopted are shown in Table 1. The code provides five-point Lagrange interpolation. It is important to have a consistent method such as this for computing the hydrogen density of both

TABLE 1

Apparent Molal Volume of PuO_2 in Nitric Acid Solution

Moles Pu/ℓ	*Apparent Molal Volume, cm³*
0	- 10.3
0.5	2.7
1.0	7.3
1.5	9.5
≥ 2.0	10.3

the solutions involved in critical experiments and those involved in any parametric study from which minimum critical masses and dimensions and corresponding limits are derived. It is also important that the method be fairly accurate if bias established from correlations with solution data is to be applied to other systems such as oxide-water mixtures. With this approach, the composition data required for $Pu(NO_3)_4$ solutions are the plutonium concentration, the plutonium isotopic composition, the total nitrate concentration, and the temperature. The code then computes the solution density and the hydrogen density.

This approach was considered preferable to the use of density data reported for the critical experiments, with hydrogen density obtained by difference and thereby containing the cumulative error, and to the use of density formulas in view of the lack of agreement among those that have been proposed by others.

One of the earlier ones is[11]

$$\rho = 1 + 0.031\ H + 0.00146\ C$$

where H is the free acid molarity and C is the plutonium concentration in g/ℓ. French work[12] covering the concentration range 12 to 166 g/ℓ, the acid molarity range 1.51 to 2.16M, and a temperature range from 20°C to 50°C resulted in the formula

$$\rho = d + 0.034\ H + 0.00147\ C$$

where d is the density of water at the appropriate temperature. From a least squares analysis of the density of a large number of $Pu(NO_3)_4$ solutions, Richey[13] derived the following expression for the concentration of water:

$$H_2O(g/\ell) = 1000 - 0.3619\ g\ Pu/\ell - 24.6\ H$$

He later corrected the coefficient of acid molarity to 33.1 (Reference 14). From the corrected expression, the formula derived for the density of $Pu(NO_3)_4$ solutions is

$$\rho = 1 + 0.0299\ H + 0.001675\ C$$

(Before correction, the acid molarity coefficient was 0.0384). The acid molarity coefficient is suspect, however. For aqueous solutions of nitric acid, the coefficient at 20°C is 0.0338 as determined by densities at 0 and 0.81M, 0.0314 as determined by densities at 0 and 7.9M, but the density is obviously not strictly a linear function of molarity. For a solution containing 160 g Pu/ℓ and 2.2 molar acid, the densities obtained from Richey's corrected formula and from the French differ by about 2%; the corresponding difference in k_{eff} calculated for a critical water-reflected sphere is about 0.01.

Once the macroscopic cross sections for a mixture are computed, they are placed in JOSHUA records that serve as input for ANISN, KENO, or any other program. A fission spectrum characteristic of the mixture accompanies the cross sections. For plutonium compounds, the spectrum is that given in Table IV of Reference 6. (With some inconsistency, the ^{239}Pu cross sections in the upper groups correspond to those in Table III of Reference 6 rather than Table IV.) A B_1 calculation, which for linearly anistropic cross sections is exact, is performed for the mixture to determine for fissionable mixtures the critical buckling and the buckling corresponding to any specified value of k_{eff} other than unity, the migration areas, and the neutron multiplication constants k. For non-fissionable mixtures, only the migration area at zero buckling is calculated. HRXN, in conjunction with transport theory calculations performed by ANISN, constitutes a second method of computation.

GLASS

GLASS[4] is basically a replacement for HAMMER[15], incorporating improvements and supercell (cells consisting of groups of dissimilar fuel and target assemblies) capability. It is adaptable to any group structure, but extensive cross-section libraries exist only for a 37-group structure and the HAMMER 84-group structure (54 MUFT groups, 30 THERMOS groups). The HAMMER group structure was used in the present work. The Standard GLASS Cross Section Library is essentially the HAMMER Library. Other libraries are provided for GLASS, however. A special library contains cross sections for H, ^{10}B, N, O, Al, Fe, and uranium and plutonium isotopes processed by ETOJ and FLANGE[16] from ENDF/B-IV files. Another special library contains, among other nuclides, cross sections for C processed from ENDF/B-III. Wherever these nuclides appear in mixtures, in the experiments with which correlations were made, their cross sections were taken from these special libraries rather than from the Standard Library. For other nuclides (Cr, N, ^{241}Am), the cross sections were taken from the Standard Library. In the special ENDF/B-IV Library, the scattering matrices of the light elements are expanded in Legendre polynomials through P_2, the heavy elements through P_1. The C cross sections are expanded only through P_1.

GLASS is intended principally for lattices. Cell fluxes are computed by integral transport theory with isotropic scattering. However, it also can treat homogeneous systems for which the functions it performs are the selection of cross sections from designated libraries, the formulation of mixtures, the computation of resonance reaction rates (by the Nordheim method), and the computation of critical buckling, k, and migration area by B_1. GLASS can collapse cross sections, but only with scattering limited to P_0. The few-group cross sections are in a form suitable for diffusion theory codes, and the number of groups is limited to 10. As it

stands, GLASS is not suitable for use with transport theory codes that permit anisotropic scattering, and there is some question[1] as to whether its diffusion theory constants are in proper form, particularly for small systems. However, its access to ENDF/B-IV cross sections and its calculation of resonance reactor rates are features that are desirable to incorporate in a computational method used for criticality safety evaluations. A special module has accordingly been written for GLASS for processing cross sections, and a special module has been written for the driver subsystem KOKO to facilitate the preparation of input and to operate on GLASS output.

Besides eliminating minor cross section inconsistencies through adjustments in self-scatter cross sections, the principal function of the special GLASS module is to implement the extended transport approximation with scattering limited to P_1, as in the Hansen-Roach set of cross sections.[6*] Scattering for the heavier elements (A >27) is limited to P_0. For plutonium isotopes, scattering at high energy is largely forward, and the ordinary transport approximation was thought to be superior to the extended approximation with P_1 scattering. For the lighter elements, scattering is limited to P_1. The value of σ_2 required for the extended transport approximation is obtained from library cross section records if they extend to P_2; otherwise, it is obtained from σ_1 and the ratio of σ_2/σ_1 for isotropic scattering in the center of mass system. Another function of the special GLASS module

---

* The scattering cross section as a function of the cosine of the scattering angle may be represented as an expansion in Legendre polynomials.

$$\sigma(\mu) = 1/2 \sum_{\ell=0}^{\infty} (2\ell + 1)\ \sigma_\ell\ P_\ell\ (\mu)$$

The extended transport approximation involves setting $\sigma_\ell = \sigma_k$ for all $\ell > k$. The expansion then becomes

$$\sigma(\mu) \simeq 1/2 \sum_{\ell=0}^{k-1} (2\ell + 1)\ (\sigma_\ell - \sigma_k)\ P_\ell\ (\mu) + \sigma_k \sum_{\ell=0}^{\infty} (2\ell + 1)\ P_\ell(\mu)$$

Expansion of the delta function $\delta(\mu-1)$ in Legendre polynominals shows that the second sum on the right is $\sigma_k\ \delta(\mu-1)$. Since this represents purely straight-ahead scattering with no energy loss, it may be disregarded. If k = 1, $\sigma_k = \bar{\mu}\sigma_0$, and the ordinary transport approximation is obtained. If k = 2, $\sigma_k = \dfrac{3\bar{\mu}^2 - 1}{2}\ \sigma_0$.

is to furnish cross sections for transfer to adjacent groups in the thermal region for heavy isotopes. The transfer cross sections for these isotopes as contained in the libraries are zero. The removal cross section is computed as $\xi\sigma_s/\Delta\mu$, and the apportionment between up and down scatter is determined by the principle of detailed balance.

Subroutines written for KOKO to supply input for GLASS write all the input records required by GLASS for a series of mixtures from a single KOKO input record. Mixtures are formulated as in HRXN, and the nitric acid tables and apparent molal volumes of PuO_2 are incorporated in the subroutines.

Subroutines written for KOKO to operate on GLASS output convert resonance reaction rates calculated by GLASS for each group to absorption and fission cross sections as outlined in Appendix A (GLASS carries the reaction rates through its B_1 calculation and finally converts them to cross sections in the process of collapsing groups). Following the conversion of resonance reaction rates to cross sections, additional subroutines written for KOKO perform the B_1 calculation and collapse cross sections as desired. GLASS already contains a B_1 calculation, but it was felt that collapsing could be implemented more easily if resonance reaction rates were first converted to cross sections. The conversion appears to be equivalent to the procedures followed in GLASS since Legendre flux moments and the critical buckling calculated by the KOKO B_1 calculation agree well with those calculated by GLASS. However, the GLASS B_1 calculation is not usually performed since it represents an unnecessary duplication.

The KOKO B_1 calculation is similar to that in HRXN and yields the buckling corresponding to a specified k_{eff} (the critical buckling if $k_{eff} = 1$), k (the ratio of production to absorption), two values of migration area (the second, computed as $(k-1)/B^2$, provided as a check on consistency), and Legendre flux moments ϕ_0 (flux), ϕ_1 (current), and ϕ_2. The moments are used as weighting functions in generating few-group cross sections. The weighting is as follows:

- $\nu\Sigma_f$, Σ_a, and Σ_{oij} $(i \neq j)$ are weighted by ϕ_o.
- Σ_{1ij} $(i \neq j)$ are weighted by ϕ_1.
- For few-group cross sections with isotropic scattering, Σ is determined from the transcendental equation relating ϕ_o and ϕ_1.
- For few-group cross sections with linearly anisotropic scattering, Σ is determined from the transcendental equation relating ϕ_1 and ϕ_2.

- Σ_{oii} is determined by difference from Σ, Σ_a, and the sum of Σ_{oij} $(i \neq j)$.

- Σ_{lii} is determined by balancing first-order sources and removals.

Options are provided for weighting by the spectrum from the previous case (in which event Σ and all Σ_{lij} are weighted by ϕ_l) and for removing upscatter in such a manner as to preserve the Legendre flux moments.

The weighting scheme ensures the same buckling, migration area, and k with the few-group cross sections as were obtained with the 84-group cross sections. This is confirmed by repeating the B_l calculation with the few-group set. The cross sections are placed in JOSHUA records in the format specified for KENO. A fission spectrum characteristic of the material is included.

Any structure may be selected for few-group cross sections. The one chosen for the standard method and for correlation with experiment is as close to the Hansen-Roach structure as is possible with the 84-group boundaries. Since upscatter increases ANISN computing time by a factor of nearly 2 and occasionally results in failure to converge and since the difference in bias with or without it is small, upscatter was removed. Cross sections for core materials were collapsed at critical buckling (unadjusted for bias). Cross sections for water or Plexiglas™ reflectors were collapsed at zero buckling. A plutonium-239 fission source was used. Cross sections for container walls were collapsed with reflector spectrum. It is questionable whether the B_ℓ spectrum generated in a nonmoderating core is the appropriate one to use for collapsing cross sections at all energies when the core is surrounded by a moderating reflector. For example, for a sphere of plutonium metal immersed in water, the B_ℓ spectrum for plutonium may be appropriate for the high-energy groups, but the influence of the H_2O reflector should be taken into account for the low-energy groups. Provision has been made for weighting metal (or oxide) cross sections by the spectrum developed at zero buckling in a metal-moderator mixture. This weighting is done in the same manner that cross sections for a material are weighted by a previous spectrum (i.e. Σ is not derived from a transcendental equation but is weighted in a straight-forward manner). The cross sections for the metal can then be taken as a combination of those determined from the B_ℓ spectrum in the metal in the high-energy groups and those weighted by the metal-moderator spectrum in the low-energy groups. The arbitrary choice made was to use a 1:1 by volume metal (or oxide) - water mixture to generate cross sections for the lower 10 groups.

ANISN

Changes in the SRL version of ANISN[2] have consisted principally of converting the code to a JOSHUA[4] module. The transverse dimension specification and search have been converted to transverse buckling; but this is not commonly used because of inconsistencies and was not used in the present work. Subroutines have been written for KOKO to prepare input for ANISN for the types of problems commonly encountered in criticality safety applications. Completely symmetric quadrature sets[17] satisfying even moments conditions are incorporated for orders 4, 8, and 16. All three were used, and extrapolation to S_∞ was carried out by the formula

$$p_\infty = \frac{32p_{16} - 12p_8 + p_4}{21}$$

which is obtained by fitting a third order polynomial in the reciprocal of the order of quadrature to values of p_n calculated by S_n with the requirement that the slope be zero when the reciprocal is zero. The parameter p may be any parameter calculated by S_n: k_{eff}, radius, etc. Use of the formula is of course not exact, but is preferable to graphical extrapolation since it is unequivocal. The formula was applied to a group of three two-group bare slab analytical benchmark problems.[18] For the thickest slab, k_{eff} calculated by S_4, S_8, and S_{16} was 0.9898, 0.9975, and 0.9991. The formula gives 0.9995 at S_∞ compared to an exact value of 1.0000. For the middle slab, the S_4, S_8, and S_{16} results were 0.7496, 0.8896, and 0.9597, respectively. The formula gives 0.9898 at S_∞, compared to 1.0000. Graphical extrapolation to 1.0000 appears reasonable, but so does extrapolation to 0.9898. However, the variation with quadrature here is much larger than that encountered in any correlations, where the maximum spread between S_4 and S_{16} is about 0.02. (Even the thickest of the three benchmark slabs bears little resemblance to a physically realizable reactor; for it, ν would have to be about 16.) For a series of 16 one-group benchmark calculations for slabs and spheres, with isotropic scattering and with c extending from 1.01 to 1.6,[19] the maximum deviation from unity of k_{eff} extrapolated to S_∞ was -0.0010 for one of the slabs. The absolute value of the deviation was <0.0005 in ten cases.

To provide a standard method for assigning spacial mesh in ANISN, KOKO assigns interval widths ΔR according to a formula proposed by Westinghouse Astronuclear Laboratory in the manual[20] that accompanied the version of ANISN received from RSIC:

$$\Delta R < \frac{1.0 + \Sigma^{o}_{g \to g} / \Sigma_g}{4\Sigma_g}$$

Where g is the group in which Σ has its maximum value. This formula can result in an excessively large number of intervals, however. In such cases, a scheme, based on several criteria[20] has been provided in KOKO that assigns a variable mesh. It assigns the finest mesh (in accordance with the formula) within subzones next to internal boundaries, where the flux is expected to vary most rapidly, and assigns successively coarser mesh (by factors of 2) away from these boundaries. Subzones within a medium all have the same number of intervals, and the default option, which was selected in the present work, limits the number to 10. This scheme has been investigated for a D_2O reflected sphere of uranium-235 dissolved in D_2O and for a water reflected plutonium metal sphere and gave good results.

SPBL

A module SPBL has been written for applying ANISN results to two- or three-dimensional bodies with separability of the neutron flux into a product of spacial components assumed. An ANISN k_{eff} search is performed for each dimension with the other dimensions assumed infinite, i.e., with zero transverse buckling. The two (finite cylinder) or three (cuboid) values of k_{eff} are supplied to SPBL together with the macroscopic cross sections of the core material. For each value of k_{eff}, a B_1 calculation is made to determine the corresponding buckling, which is interpreted as the geometric buckling. If desired, extrapolation distances may be calculated (by hand), and they appear quite reasonable. The geometric bucklings are combined, and k_{eff} is calculated (again by B_1) for the body. For large bodies, this approach is quite good since geometric bucklings are determined largely by the dimensions. For small bodies, it tends to overestimate k_{eff}. For a series of bodies, with the same or similar core material, in which a dimension is progressively reduced, the critical transverse buckling is correspondingly reduced. Extrapolation to zero transverse buckling then yields k_{eff} for a critical infinite cylinder or infinite slab.

KENO

In principle, Monte Carlo and S_n transport theory calculations extrapolated to S_∞, performed with the same cross sections, should be equivalent methods, and some Monte Carlo calculations as carried out by KENO were done to supplement ANISN calculations. Changes in the SRL version of KENO-IV have consisted principally of converting it to a JOSHUA module. Some redundancy in input was removed, and some simplifications were achieved in the process. Mixing tables were removed, and macroscopic cross sections are expected to be contained in JOSHUA records. Presently, Hansen-Roach cross sections as prepared by HRXN and ENDF/B-IV cross sections as processed to 16 groups by GLASS are used. In the present study, KENO was used principally to supplement results obtained with SPBL and to assist

in the extrapolation to infinite bodies. The number of neutrons per generation was always specified as 300. Values of k_{eff} are based on at least 60 generations (18,000 neutrons), generally 100 generations. Adjoint biasing, as furnished with KENO-IV was used in the hydrogenous reflectors. (The small differences in group boundaries for the GLASS cross sections were assumed not to invalidate the weights.) When compared with the set of one-group benchmark calculations to which ANISN was applied,[19] KENO gave good results. For the eight slabs and eight spheres, k_{eff} was within one standard deviation of unity in 9 cases, within two in 5 cases, and within three in the remaining 2. There were five underpredictions. The two cases slightly exceeding two standard deviations were on either side of unity. On the bases of the one-group comparisons, both KENO and ANISN solve the transport equation with acceptable accuracy and may be considered equivalent. Recently, what was considered to be an error in the treatment of P_1 scattering in KENO was discovered at ORNL.[21] Calculations were made both without and with the proposed correction, which randomizes the scattering angle.

EXPERIMENTAL DATA

Many critical experiments have been performed with plutonium. Paxton[22] cites some ten references to critical experiments with aqueous solutions and fifteen to experiments with metal. From the vast number of experiments in these and other references, Durst, et al. have somewhat arbitrarily selected thirty-three to serve as benchmarks.[23] However, in the present work, the principal interest is in experiments with one-dimensional systems, such as spheres and cuboids and finite cylinders that can readily be extrapolated to infinite slabs and cylinders or that fill in gaps in the data even if separability is assumed in analyzing them. To cover all the parameters involved in the experiments, all such available experiments should be calculated, particularly with one-dimensional computer programs that do not consume large amounts of computer time. Accordingly, many more experiments were included in the present study than in Durst's compilation, but on the other hand, not all in his listing. In particular, the French and British experiments with cylinders and cuboids were omitted. Some experiments dealt with special reflectors such as concrete, paraffin, and cadmium, but these were not considered of interest at this time. A survey was made of both Nuclear Science and Engineering and Nuclear Technology to see whether any experiments had been omitted by Paxton or Durst. The original publications and Durst's compilation were studied carefully in arriving at the experimental conditions used as input for the computer codes.

$Pu(NO_3)_4$ Solution

The earliest sphere experiments (P-11 project) were performed with $Pu(NO_3)_4$ solutions contained within thin spherical shells

of stainless steel except for one shell of aluminum.[24] Nominal diameters for water-reflected spheres were 11, 12, 13, 14, and 15 inches. A bare sphere 16 inches in diameter and one 18 inches in diameter covered with 0.02-inch cadmium were included. Some sphere experiments were performed in which phosphate, bismuth, manganese, or lithium were present, but these and the cadmium-covered spheres were not considered of interest in the present study, and no correlations were made. In the sphere experiments, the reported critical masses are not exactly the product of the reactor volume and the reported concentration, due presumably to a correction made for the control rod and perhaps for the sphere neck. In the listings of the experimental data in Table 2, the plutonium concentrations are the quotients of the reported critical masses and the sphere volumes. In this and subsequent tables, the plutonium isotopic composition is given in weight percents of isotopes other than plutonium-239. The weight percent plutonium-239 is obtained by difference from 100. Radii are calculated from volumes. Where experiments appeared to be duplicate runs, averages were taken. The reported experimental uncertainties are small. The critical masses are estimated to be within $\pm 1.5\%$, the sphere volumes within $\pm 0.3\%$, the nitrate ion concentrations within $\pm 0.6\%$, and the percentages of plutonium-240 within $\pm 7\%$. Densities calculated from nitric acid tables and the apparent molal volumes of Table 1 were generally less than the reported values. The maximum underestimate was 1.27%; the next largest, 0.82%; and the maximum overestimate, 0.31%. On the average, the density was underestimated by 0.20%.

The first experiments in the P-11 Project were with water-reflected cylinders, and, although separability must be assumed in analyzing the experiments by one dimensional methods, some correlations were made to establish the validity of applying bias determined with spheres to calculations for infinite cylinders. Not all the experiments were included; experiments were omitted in which temperature was a variable and in which an extra thickness of steel sheet surrounded the cylinder. Temperature was slightly more variable than in the sphere experiments, but variations were not taken into account in the correlations. Many of the reported nitrate concentrations were estimates, due perhaps to an initial failure to recognize its significant bearing on critical mass. The cylinders were reflected on all surfaces. The critical conditions are given in Table 3. The discrepancy between calculated and reported densities was larger for these experiments, with more scatter, ranging from an underestimate of 1.55% to an overestimate of 0.83% and averaging out to an underestimate of 0.45%.

Results of a second series of critical experiments with spheres of $Pu(NO_3)_4$ solutions, performed at Hanford at the Critical Mass Laboratory beginning in about 1961, were published in 1966.[8] An analysis of these experiments and the P-11 Project experiments was published in 1968[13] and contained some data not in the earlier publication. Besides continuing the P-11

TABLE 2

Critical Spheres of $Pu(NO_3)_4$ Solution
(P-11 Project)

Reflector	*Radius, cm*	^{240}Pu, *wt %*	*Pu/ℓ, g*	NO_3^-*/ℓ, g*	*Fe/ℓ, g*[a]	*Temp, °C*
H_2O[b]	13.95[c]	3.12	135.8[d]	229.0	0.464	27
	15.36	3.12	50.16	138.5	0.189	27
			51.74	163.0	0.272	27
			56.42	207.0	0.245	27
			59.97	237.0	0.192	27
			63.66	270.0	0.197	27
			70.44	322.0	0.218	27
			77.42	359.0	0.237	27
	16.27[e]	3.12	36.25	93.1	0.114	27
			37.08	125.0	0.128	27
	16.54	1.76	33.55	86.7	0.124	27
			34.58	116.5	0.177	27
			35.37	145.0	0.124	27
		3.12	37.70	130.0	0.103	27
			38.38	156.0	0.141	25
			40.92	205.0	0.257	27
			44.35	269.5	0.266	27

a. Fe assumed present as Fe_2O_3 with density 5.24 g/cm^3.

b. H_2O thickness ≥12 inches.

c. Except where noted to the contrary, solution was enclosed by Type 347 stainless steel shell. Composition assumed was 70% Fe, 18% Cr, 12% Ni with density 8.0 g/cm^3. Thickness was 0.05 in (0.127 cm).

d. This solution was subcritical by an unknown amount.

e. Solution enclosed by aluminum shell. Density assumed to be 2.7 g/cm^3. Thickness was 20 gauge (0.081 cm).

TABLE 2 (Cont)

H_2O	17.80	0.54	26.48	77.8	0.145	27
			26.50	107.0	0.149	27
			27.39	137.5	0.156	27
			28.28	187.5	0.164	27
		1.76	27.77	109.5	0.094	27
		3.12	28.81	87.4	0.110	27
			29.72	111.3	0.123	27
			30.16	143.0	0.113	27
			31.81	208.0	0.120	27
			35.55	309.5	0.145	27
			39.55	408.0	0.147	27
		4.05	29.86	87.49	0.128	27
			30.73	119.3	0.079	27
			31.64	146.8	0.086	27
			33.76	210.7	0.097	27
			36.25	272.4	0.104	27
			38.71	335.2	0.126	27
			41.12	384.9	0.126	27
		4.40	30.80	126.5	0.108	27
			32.06	158.0	0.102	27
	19.06	3.12	24.97	116.0	0.088	27
			25.73	147.0	0.094	27
			27.15	212.0	0.096	27
None	20.13	4.15	35.59	106.9	0.112	23
			38.13	163.0	0.124	24
			38.16	180.0	0.178	23
			43.43	281.8	0.179	22

TABLE 3

Critical Water-Reflected Cylinders of $Pu(NO_3)_4$ Solution[a]
(P-11 Project)

Radius, cm	*Height, cm*	^{240}Pu, *wt %*	*Pu/ℓ, g*	*NO_3^-/ℓ, g*	*Fe/ℓ, g*
10.16	48.29[b]	2.85	77.40	152.0	0.644
11.43	29.87	2.83	109.16	166.0	0.395
	30.71	2.83	99.09	136.5	0.378
	32.33	2.83	85.14	151.0	0.321
	35.41	2.83	73.92	125.6	0.231
	40.08	2.83	61.49	134.0	0.303
	44.58	2.83	54.33	119.8	0.257
12.70	25.22	2.85	77.40	152.0	0.644
	24.74	2.85	76.93	152.0	0.327
	27.25	2.85	62.47	146.0	0.269
	32.69	2.85	49.26	142.0	0.260
	41.76	2.85	39.10	138.0	0.172
13.97	22.81	2.90	63.99	121.1	0.298
	25.96	2.90	48.98	139.0	0.238
	27.08	2.83	47.21	117.0	0.275
	32.64	2.83	41.73	215.0	0.255
	31.19	2.85	39.10	138.0	0.172
	43.00	2.83	36.90	300.0	0.263
	39.55	2.85	33.54	137.0	0.193
	47.12[c]	2.85	30.81	136.0	0.173
15.24	17.32[c]	2.83	109.16	166.0	0.395
	22.35	2.90	48.75	116.3	0.223
	25.25	2.90	42.29	126.6	0.174
	28.47	2.90	36.52	107.1	0.161
	33.43	2.90	31.14	114.0	0.153
	44.45	2.90	26.45	134.0	0.154

a. Solution temperature 27°C. Solution enclosed by stainless steel, with composition of Table 2, 0.062 in. (0.16 cm) thick.

b. Subcritical by an unknown amount.

c. "A reliable extrapolation to the critical height was made." Experiment was subcritical.

Project series, these experiments investigated the effect of concrete, stainless steel, and paraffin as reflectors, but the latter are not included in the present listings. The experimental conditions are listed in Table 4. The sphere radii, derived from volumes, have been modified to take account of an empirically determined correction for the vessel neck. For the fourteen experiments reported by Lloyd et al. (Richey reported no densities), calculated densities again generally underestimated reported densities ranging from an underestimate of 1.03% to an overestimate of 0.21% and averaging out to an underestimate of 0.38%. An analysis of the experimental error by Lloyd et al. led to an estimate of an uncertainty of about +1% in the critical mass except for the two experiments where Pu($\overline{V}$I) and polymer were present, where the uncertainty was estimated to be $\pm$5%.

The only other experiment with spheres was a recent one[25] utilizing the large sphere of Gwin and Magnuson[26] in order better to establish the minimum critical concentration of plutonium-239. In the paper, as presented at the ANS meeting (a copy of which was distributed at the meeting), solution analyses from two different sources were presented, differing by about 1.5%. In a preview of the paper to be submitted for publication, data from the first of these sources are omitted since they were considered to be of poorer quality. No nitrate concentration was reported; it was inferred from the valency of Pu(IV) and from the reported HNO_3 molarity. The critical concentration was interpolated from extrapolations to critical volumes that bracketed the actual volume of the sphere. Table 5 gives the critical conditions as determined by the two sets of measurements. The critical plutonium concentrations were determined from a power fit to the data. Linear interpolation of the concentrations for the critical volumes on either side of the actual volume appears equally valid and leads to 9.618 and 9.457 g Pu/ℓ for the two sets of measurement. (The acid molarities are linear interpolations.) Densities calculated from Table 1 and nitric acid tables underestimate the reported densities by 0.11 and 0.22%, but densities calculated from reported atom densities underestimate the reported solution densities by 0.25 and 0.40%.

A series of experiments has been performed in a slab tank of adjustable thickness, both bare and reflected by water.[27] Plutonium containing about 5% plutonium-240 and some containing about 20% plutonium-240 were used. The data have been extrapolated to completely bare infinite slabs and to infinite, water-reflected slabs with no intervening wall. The extrapolated critical conditions are listed in Table 6. Sizable corrections were required for tank walls and support structure and, for the bare slabs, room return. Extrapolation to infinite slab thickness was based on buckling conversions made from bucklings and extrapolation distances determined from several pairs of thickness and critical height measurements for each composition. The experimenters estimate an uncertainty of $\pm$0.2 cm in the infinite slab thicknesses. Although

TABLE 4

Critical Spheres of $Pu(NO_3)_4$ Solution
(Critical Mass Laboratory)[a]

Reflector	*Radius, cm*	*Wall, cm SS*	*Pu/ℓ*[b], *g*	*NO_3^-/ℓ, g*
Water	14.55	0.125[c]	73.0	86
			74.5	105
			96.0	203
			100.0	230
			119.0	245
			126.0	262
			132.0	281
			140.0	284
			269.0	346
			295.0[d]	303
			435.0[d]	372
	17.67	0.112	33.0	162
			33.2	164
			38.4	292
			38.6	292
			39.2	313
			47.5	462
			47.9	465
	19.29	0.122	24.4	58
			38.7	517
None	19.45	0.122	39.0	64
			172.3	486

a. Solution temperature 25° C.

b. Pu contained 4.57% ^{240}Pu, 0.31% ^{241}Pu by weight.[23]

c. Assumed to have the same composition as in Table 2.

d. Contained Pu(VI) and polymer.

TABLE 5

Critical Bare Sphere of Low Concentration Pu Solution[a]

Radius, cm	*Wall*	*Pu/ℓ[b], g*	*NO_3^-/ℓ, g*
61.00	0.77 cm Al	9.598[c]	68.801
		9.426	78.294

a. Solution temperature 23°C.

b. Pu contained 0.004% ^{238}Pu, 2.521% ^{240}Pu, 0.075% ^{241}Pu, 0.014% ^{242}Pu by weight.

c. Omitted from later report as being less reliable.

TABLE 6

Critical Infinite Slabs[a]

Isotopic Composition, wt %				*Infinite Slab Thickness, cm*			
^{238}Pu	*^{240}Pu*	*^{241}Pu*	*^{242}Pu*	*Bare*	*H_2O Reflected*	*Pu/ℓ, g*	*NO_3^-/ℓ, g*
0.006	4.671	0.255	0.009	16.91	9.13	58	203
				17.99	9.78	58	397
0.19	18.400	4.53	0.96	19.79	11.38	66.5[b]	219
				20.05	11.21	160[b]	360
				21.48	11.64	241[b]	495
					13.01	412[b]	664
0.07	23.185	3.958	0.966	21.19	11.70	202[c]	313
					12.43	284[c]	436

a. Temperature 23°C.

b. ^{241}Am/Pu weight ratio 0.0028. Am was assumed present as AmO_2 with density 11.6 g/cm^3. Where no cross sections were available for ^{241}Am (MGBS and HRXN), it was mocked up by B with 0.0492 g B assumed equivalent to 1 g ^{241}Am. B was assumed present with density 10^6 g/cm^3.

c. ^{241}Am/Pu weight ratio 0.0021.

not as precise as the sphere experiments, the slab experiments are useful in indicating whether bias determined with spheres is appropriate for slabs and in indicating the effect of large isotopic concentrations of plutonium-240 on the bias. Solution densities are not given in the final report of the experiments,[27] but are given in various Battelle reports issued during the course of the experiments (BNWL-340, BNWL-775, BNWL-921, and BNWL-1053). Calculated densities, with americium-241 assumed present as AmO_2 with density 11.6 g/cm^3 agreed well with reported densities, ranging from an underestimate of 0.02% to an overestimate of 0.52%.

Some experiments in cylinders, water-reflected on sides and bottom, bare on top, have been performed with plutonium containing larger concentrations of plutonium-240 than those in the sphere experiments. These experiments are useful for indicating the bias to be used in calculating limits for systems with high plutonium-240 concentrations, although the assumption of separability or the application of Monte Carlo to the experiments introduces some uncertainty. In a series of experiments to determine the poisoning effect of Raschig rings,[10] one experiment was performed without rings. Similarly, in a series in which the poisoning effect of Gd was studied, one experiment was performed without gadolinium.[28] (Incidentally, the reported isotopic composition sums only to 99.96%; a slightly modified composition[23] summing to 100% was used in calculations and is the one given in Table 7.) Finally, a series of experiments was performed with high-burnup plutonium containing about 43% plutonium-240.[29] Some gadolinium was present in these experiments, persisting from previous experiments. The critical conditions are given in Table 7. Densities were reported only for the Raschig ring and gadolinium experiments. Calculated densities agreed with reported densities ranging from an underestimate of 0.63% to an overestimate of 0.38% and averaging out to an underestimate of 0.04%.

PuO_2 - Plastic Compacts

The practical upper limit on plutonium concentration in plutonium nitrate solutions is about 500 g/ℓ corresponding to a H/Pu ratio of about 50. To fill in the gap between metallic plutonium and nitrate solutions, several groups of experiments have been performed with assemblies built of homogeneous PuO_2 - polystyrene compacts, both bare and reflected by Plexiglas™. In one series of experiments, assemblies were built with essentially dry blocks of PuO_2. Reflected assemblies were built with varying heights so that extrapolations could be made to infinite slabs. Empirical corrections were made for the materials cladding the blocks and for stacking voids; therefore, the published results apply to homogeneous cuboids and infinite slabs. The experiments are listed here in chronological order.

The first experiments were performed with compacts having a H/Pu ratio of about 15.[30] Two plutonium compositions were

TABLE 7

Critical Cylinders[a]

Isotopic Composition, wt %							
^{238}Pu	^{240}Pu	^{241}Pu	^{242}Pu	Radius, cm	Ht, cm	Pu/ℓ, g	NO_3^-/ℓ, g
0.022	8.322	0.897	0.049	15.263	28.804	275.0	480.0
0.004	8.383	0.851	0.049	30.514	15.44	116.0	238.9
0.2	42.9	10.8	4.7	30.514	54.70	140.0[b]	457.6
					50.55	116.0[b]	378.0
					48.26	99.3[b]	331.4
					47.00	85.5[b]	282.8
					47.29	75.6[b]	248.9
					49.12	65.1[b]	217.5
					52.83	56.3[b]	186.0
					63.47	46.8[b]	154.3
					80.92	40.6[b]	133.0

a. Temperature was assumed to be 23°C. Cylinder walls were stainless steel 0.079 cm thick with composition assumed the same as in Table 2. The bottom was 0.95 cm thick. Cylinders were water reflected on sides and bottom, bare on top. The vessel had a 0.95-cm-thick steel cover, and the water reflector extended to the top of the vessel. The inside height of the vessel was about 105 cm (There are small discrepancies in the references).

b. ^{241}Am and Gd present at 1.08 and 0.0089%, respectively, of Pu concentration. Am assumed present as AmO_2 with density 11.6 g/cm^3, Gd as Gd_2O_3 with density 7.407 g/cm^3. Where no ^{241}Am cross sections were available, ^{241}Am was mocked up by B as in Table 6. With some inconsistency, B was assumed present as B_2O_3 with density 2.17 g/cm^3, its apparent density in boric acid.

used, one containing 2.2% plutonium-240, the other 8%. One nearly cubic bare assembly was made critical with each composition. The corrected dimensions were 30.68 x 30.68 x 32.84 ±0.52 cm at 2.2% plutonium-240, 35.63 x 35.63 x 36.04 ±0.60 cm at 8.0% (Reference 23 erroneously gives 34.49 cm for the third dimension at 2.2%). A calculated bare extrapolation distance, together with the assembly dimensions, yielded a buckling for each of these assemblies. Equating the buckling to the usual geometric buckling expression for a cuboid (assuming separability), and assuming the same extrapolation distance for all three dimensions permitted the extrapolation distance to be determined for each of the critical reflected assemblies that was built with each composition. Extrapolation to zero buckling transverse to the dimension being reduced yielded the extrapolation distance appropriate for an infinite reflected slab and hence the slab thickness. The thickness reported for the infinite bare slab resulted from a calculated extrapolation distance slightly smaller than that calculated for the cube and is perhaps somewhat more uncertain than that reported for the reflected slab. Significantly lower calculated reactivity at 8% plutonium-240 led the experimenters to search for the cause and to investigate the effect of PuO_2 particle size. The experimental results were corrected to homogeneous systems based on an average of the maximum and minimum possible effects of particle size.[31] Both the original and corrected infinite slab dimensions are given in Table 8.

The next group of experiments[32] was performed with compacts in which the H/Pu ratio was 5. The plutonium-240 concentration in the plutonium was 11.46%. These experiments were performed essentially in the same manner as those at H/Pu = 15, with a single, nearly cubic bare assembly and several reflected assemblies. The corrected dimensions of the bare assembly were 35.84 x 35.84 x 28.82 ±0.05 cm. The infinite reflected slab thickness was determined both from a linear extrapolation of a plot of extrapolation distance for reflected assemblies against transverse buckling and from a linear extrapolation of critical thickness against inverse cross sectional area. The two methods agree within the error limits reported. Particle size was smaller than at H/Pu = 15, and was concluded not to have a significant effect.[31] The experiments are described in Table 9. The composition was reported only as atom densities. The reflected assembly dimensions were taken from Reference 23; the corrected dimensions are not given in Reference 32.

The third group of experiments was performed with blocks made of essentially dry PuO_2 (H/Pu = 0.04).[33] The plutonium-240 concentration in the plutonium was 18.35%. Temperature variations of as much as 30°C were a problem in performing the experiments; count rates were corrected to 50°C. There was insufficient fuel to make a bare assembly critical, but two bare assemblies were

TABLE 8

PuO_2 - Polystyrene Compacts at H/Pu = 15

Isotopic Composition, wt %			*Density*	*Wt %*		*Infinite Slab Thickness, cm*		
^{240}Pu	*^{241}Pu*	*^{242}Pu*	*g/cm³*	*PuO_2*	*CH*[a]	*Bare*	*Reflected*[b]	*Ref*
2.20	0.11		2.200	58.0	42.0	16.09 ± 0.41	5.99 ± 0.10	30
						15.96 ± 0.54	6.03 ± 0.14	31
8.06	0.75	0.03	2.046	58.2	41.8	18.48 ± 0.41	7.38 ± 0.09	30
						18.74 ± 0.67	7.58 ± 0.29	31

a. Polystyrene.

b. Plexiglas. Density = 1.185 g/cm³; 60% C, 32% O, 8% H by weight (Reference 23). Thickness, 15 cm.

TABLE 9

Polystyrene Compacts at H/Pu = 5

Composition, atoms/barn-cm		*Critical Reflected*[a] *Assembly Dimensions, cm*		
		L	*W*	*H*
^{239}Pu	4.986×10^{-3}	25.60	25.60	18.33 ± 0.01
^{240}Pu	6.623×10^{-4}	30.72	30.72	14.18 ± 0.02
^{241}Pu	1.382×10^{-4}	40.96	40.96	10.59 ± 0.01
^{242}Pu	1.026×10^{-5}	51.20	51.20	9.04
O	1.159×10^{-2}	*Critical Infinite Slab Thickness, cm*		
C	2.92×10^{-2}	Bare	16.83 ± 0.31	
H	2.92×10^{-2}	Reflected[a]	5.98 ± 0.10[b]	
Pu density, g/cm³	2.302		5.88 ± 0.21[c]	

a. Plexiglas as in Table 8.

b. From extrapolation distance extrapolation.

c. From critical thickness extrapolation.

built with driver regions of H/Pu = 5 material so that extrapolation to the bare critical assembly was possible. Its corrected dimensions were 30.78 x 30.78 x 20.99 ±0.22 cm. The same techniques were used in analyzing the experiments to extrapolate to the infinite reflected slab thickness as at H/Pu = 5 (except that extrapolation distance was plotted against inverse cross-sectional area rather than transverse buckling), but agreement was poorer although still within reported error limits. For these experiments, the reflected assembly dimensions corrected for voids, cladding, and temperature effects were also reported and are given in Table 10 along with composition data (given only as atom densities) and infinite thicknesses.

The final group of experiments with PuO_2 - polystyrene compacts was performed with material with H/Pu = 50.[34] (Additional experiments have been performed with mixed PuO_2-UO_2 compacts.[35]) The plutonium-240 concentration in the plutonium was 18.35%, as in the dry PuO_2 experiments. There was again insufficient fuel to make a bare array critical, and driver regions of H/Pu = 5 material were used to deduce that a bare assembly with corrected dimensions 46.08 x 40.96 x 49.12 ±0.50 cm would be critical. From these dimensions and a calculated bare extrapolation distance, a buckling was calculated which, in conjunction with corrected reflected array dimensions, led to extrapolation distances as before. Both extrapolation distances and critical heights for the reflected assemblies were plotted against inverse cross-sectional area and extrapolated to zero area. As for the dry oxide, critical dimensions of reflected assemblies, corrected for voids and cladding, are reported and are given in Table 11 along with the infinite slab thicknesses and the core composition.

Pu Metal

Three experiments with plutonium metal spheres are included in the present listing; two bare spheres of delta phase plutonium differing in the isotopic concentrations of plutonium-240[36] and a water-reflected sphere of alpha phase plutonium.[37] The critical conditions are given in Table 12. Radii were derived from reported masses and densities.

CORRELATIONS

Correlations to establish bias were made between the data in Tables 2 through 12 and the combinations of computer programs HRXN-ANISN, GLASS-ANISN, and in some cases HRXN-KENO and GLASS-KENO. Correlations were made between data for $Pu(NO_3)_4$ solutions in spheres and slabs and MGBS-TGAN to evaluate the

TABLE 10

PuO_2 Compacts

Composition, atoms/barn-cm		*Critical Reflected[a] Array Dimensions, cm*		
		L	*W*	*H*
^{238}Pu	3.383×10^{-5}	25.65	25.65	10.03 ± 0.01
^{239}Pu	1.092×10^{-2}	25.65	30.78	8.98 ± 0.01
^{240}Pu	2.654×10^{-3}	30.78	30.78	7.97 ± 0.03
^{241}Pu	7.269×10^{-4}	30.78	41.05	6.86 ± 0.08
^{242}Pu	1.632×10^{-4}	41.05	41.05	5.95
O	3.094×10^{-2}			
H	5.511×10^{-4}	*Critical Infinite Slab Thickness, cm*		
Pu density, g/cm^3	5.762	Bare		12.17 ± 0.28
		Reflected[b]		3.01 ± 0.44
				3.34 ± 0.10[c]

a. Plexiglas, as in Table 8.

b. From linear extrapolation of extrapolation distance as a function of inverse cross-sectional area. Plotting against transverse buckling extrapolates to a greater extrapolation distance and reduces the thickness to 2.85 cm.

c. From linear extrapolation of thickness as a function of inverse cross-sectional area.

TABLE 11

Polystyrene Compacts at H/Pu = 50

Composition, Atoms/barn-cm		*Critical Reflected[a] Assembly Dimension, cm*		
^{238}Pu	2.125×10^{-6}	40.72	30.54	29.64 ± 0.12
^{239}Pu	6.952×10^{-4}	40.72	40.72	23.58 ± 0.10
^{240}Pu	1.689×10^{-4}	40.72	45.81	22.06 ± 0.06
^{241}Pu	3.952×10^{-5}	50.90	45.81	19.69 ± 0.07
^{242}Pu	1.045×10^{-5}	50.90	50.90	18.68 ± 0.08
^{241}Am	7.345×10^{-6}	50.90	61.08	17.48 ± 0.05
O	2.082×10^{-3}	61.08	61.08	16.35 ± 0.06
H	4.575×10^{-2}	*Critical Infinite Slab Thickness, cm*		
C	4.505×10^{-2}	Bare		23.85 ± 0.29
		Reflected[a]		11.06 ± 0.20[b]
				10.87 ± 0.14[c]

a. Plexiglas, as in Table 8 except that atom densities specified in Reference 34 result in slightly higher material and hydrogen densities.

b. From extrapolation of extrapolation distances.

c. From extrapolation of thicknesses.

TABLE 12

Plutonium Metal Spheres

Isotopic Composition, atom %					
Reflector	*^{240}Pu*	*^{241}Pu*	*^{242}Pu*	*Radius, cm*	*Density, g/cm^3*
None	4.5	0.3		6.385 ± 0.013	15.61[a]
	20.1	3.1	0.4	6.660 ± 0.017	15.73[b]
Water[c]	5.18	0.3	0.02	4.122 ± 0.006	19.74

a. Contained 1.02% gallium by weight.

b. Contained 1.01% gallium by weight.

c. Effectively infinite. Temperature assumed to be 20°C.

magnitude of the effect of differences in data treatment from earlier correlations. The correlations are expressed as the value of k_{eff} calculated for critical assemblies. The bias is then k_{eff}-1. The uncertainties in the bias corresponding to experimental uncertainties were largely evaluated with HRXN-ANISN.

$Pu(NO_3)_4$ Solution Spheres

Correlations of HRXN-ANISN and GLASS-ANISN with the experiments of Tables 2, 4, and 5 are given in Table 13. The correlations are listed in the same order as the experiments and are identified by concentration. In the case of GLASS-ANISN, correlations were made with representative experiments rather than with the entire set.*

The S_4 HRXN-ANISN calculations for some of the experiments of Table 4 are a repetition of earlier correlations.[38] Most of the differences can be ascribed to the previous use of a fixed density of 11.46 g/cm^3 for PuO_2 in nitric acid rather than the apparent molal volumes of Table 1. Differences in temperature, interpretation of data, quadrature, and mesh point assignment also play roles, however.

The critical value of k_{eff} (1 + bias) at S_∞ is plotted against H/Fissile plutonium in Figure 1 for HRXN-ANISN and in Figure 2 for GLASS-ANISN. The curves are drawn through the more reliable point for the large sphere. Examination of the data reveals no pronounced trend as a function of nitrate concentration or of plutonium-240 isotopic concentration. The curves drawn are "eyeball" fits to the data.

Scatter about the curves provides an indication of the uncertainty in the bias. However, the effect on k_{eff} of reported experimental uncertainties was investigated with HRXN-ANISN. In the P-11 Project experiments, nitrate ion concentration was reported to be within $\pm$0.6%, percent plutonium-240 within $\pm$7%, sphere volume within $\pm$0.3%, and critical mass within $\pm$1.5%. The respective variations in k_{eff} were evaluated for selected experiments and found to range, respectively, from $\pm$0.0001 to $\pm$0.0005, $\pm$0.0003 to $\pm$0.0022, $\pm$0.006 to

---

* The S_{16} calculations were inadvertently first made with H_2O reflector group constants weighted by the uranium-235 spectrum from the Standard Library rather than by the plutonium-239 spectrum from ENDF/B-IV. Although the respective values of M^2, 32.48 cm^2 and 33.89 cm^2 at 25°C, differed appreciably, the former spectrum increased k_{eff} for reflected spheres only by 0.0004.

TABLE 13

Correlation of HRXN-ANISN and GLASS-ANISN with Pu $(NO_3)_4$ Sphere Experiments

		k_{eff}							
		HRXN-ANISN				GLASS-ANISN			
Pu/ℓ, g	$H/^{239}Pu$ [a]	S_4	S_8	S_{16}	S_∞	S_4	S_8	S_{16}	S_∞
135.8	184.5	>0.9964	>0.9922	>0.9910	>0.9906	>1.0455	>1.0414	>1.0402	>1.0398
50.16	518.8	0.9949	0.9914	0.9903	0.9899	1.0369	1.0334	1.0324	1.0320
51.74	498.3	0.9945	0.9909	0.9898	0.9894				
56.42	449.4	0.9969	0.9933	0.9923	0.9919				
59.97	417.7	0.9983	0.9946	0.9936	0.9933	1.0425	1.0390	1.0379	1.0375
63.66	388.2	0.9984	0.9948	0.9937	0.9933				
70.44	343.2	0.9983	0.9946	0.9936	0 9933				
77.42	307.2	0.9995	0.9957	0.9947	0.9944	1.0457	1.0421	1.0410	1.0406
36.25	729.7	1.0027	0.9995	0.9985	0.9981				
37.08	705.3	1.0007	0.9975	0.9965	0.9961	1.0351	1.0319	1.0309	1.0305
33.55	779.3	0.9967	0.9936	0.9927	0.9924	1.0312	1.0282	1.0272	1.0268
34.58	748.1	0.9970	0.9938	0.9929	0.9926				
35.37	723.8	0.9958	0.9927	0.9918	0.9915				
37.70	692.4	1.0001	0.9970	0.9961	0.9958	1.0354	1.0323	1.0314	1.0311
38.38	674.3	0.9987	0.9955	0.9946	0.9943				
40.92	620.2	0.9996	0.9965	0.9955	0.9951				
44.35	557.5	0.9996	0.9964	0.9955	0.9952	1.0373	1.0342	1.0333	1.0330
26.48	978.3	1.0014	0.9987	0.9979	0.9976				
26.50	967.4	0.9957	0.9930	0.9922	0.9919				
27.39	925.7	0.9977	0.9950	0.9941	0.9938	1.0266	1.0240	1.0232	1.0229
28.28	880.1	0.9952	0.9925	0.9917	0.9914				
27.77	933.8	0.9973	0.9946	0.9938	0.9935	1.0258	1.0232	1.0224	1.0221
28.81	920.0	1.0001	0.9975	0.9966	0.9963	1.0285	1.0258	1.0250	1.0247
29.72	884.2	1.0023	0.9996	0.9988	0.9985				
30.16	861.4	0.9992	0.9965	0.9957	0.9954				
31.81	796.9	0.9976	0.9948	0.9940	0.9937	1.0272	1.0246	1.0238	1.0235
35.55	684.0	0.9989	0.9961	0.9953	0.9950				
39.55	588.5	0.9973	0.9945	0.9936	0.9933	1.0307	1.0279	1.0271	1.0268
29.86	896.3	1.0013	0.9986	0.9978	0.9975	1.0295	1.0269	1.0261	1.0258
30.73	861.0	1.0011	0.9984	0.9976	0.9973				
31.64	827.9	1.0018	0.9991	0.9983	0.9980				
33.76	757.3	1.0022	0.9995	0.9986	0.9983	1.0322	1.0296	1.0288	1.0285
36.25	688.0	1.0033	1.0005	0.9997	0.9994				
38.71	627.3	1.0020	0.9992	0.9984	0.9981				
41.12	577.6	1.0017	0.9989	0.9980	0.9977	1.0350	1.0322	1.0314	1.0311
30.80	860.0	0.9976	0.9950	0.9941	0.9938				

a. Includes ^{241}Pu where specified, therefore, actually H/Fissile plutonium.

TABLE 13 (Cont)

32.06	816.6	0.9998	0.9970	0.9962	0.9959	1.0288	1.0261	1.0253	1.0250
24.97	1051	1.0008	0.9985	0.9978	0.9975				
25.73	1008	1.0021	0.9997	0.9990	0.9987	1.0258	1.0236	1.0228	1.0225
27.15	932.1	1.0019	0.9996	0.9988	0.9985				
35.59	748.7	1.0038	1.0020	1.0013	1.0010	1.0404	1.0386	1.0379	1.0376
38.13	684.6	1.0035	1.0016	1.0009	1.0006				
38.16	680.0	1.0003	0.9984	0.9977	0.9974				
43.43	574.3	0.9980	0.9961	0.9954	0.9951	1.0380	1.0361	1.0354	1.0351
73	368.9	0.9987	0.9948	0.9937	0.9933	1.0447	1.0410	1.0399	1.0395
74.5	359.1	0.9971	0.9932	0.9921	0.9917				
96	268.5	0.9983	0.9944	0.9933	0.9929				
100	255.0	0.9959	0.9920	0.9909	0.9905	1.0426	1.0387	1.0376	1.0372
119	212.8	1.0021	0.9982	0.9971	0.9967				
126	199.6	1.0016	0.9977	0.9965	0.9961	1.0478	1.0440	1.0429	1.0425
132	189.0	1.0000	0.9961	0.9949	0.9945				
140	177.9	1.0015	0.9976	0.9965	0.9961				
269	89.5	1.0072	1.0033	1.0022	1.0018	1.0470	1.0433	1.0421	1.0416
295	83.0	1.0167	1.0128	1.0117	1.0113	1.0553	1.0515	1.0504	1.0500
435	54.1	1.0135	1.0096	1.0085	1.0081	1.0483	1.0445	1.0434	1.0430
33	794.4	1.0013	0.9986	0.9977	0.9974				
33.2	789.1	1.0021	0.9994	0.9985	0.9982	1.0316	1.0289	1.0281	1.0278
38.4	648.7	1.0036	1.0008	0.9999	0.9996				
38.6	645.2	1.0045	1.0017	1.0008	1.0005	1.0363	1.0336	1.0327	1.0324
39.2	629.7	1.0028	1.0000	0.9991	0.9988				
47.5	485.1	1.0003	0.9974	0.9965	0.9962	1.0356	1.0328	1.0319	1.0316
47.9	480.3	1.0008	0.9978	0.9970	0.9967				
24.4	1115	1.0042	1.0020	1.0013	1.0010	1.0262	1.0240	1.0233	1.0230
38.7	577.9	1.0058	1.0033	1.0025	1.0022	1.0351	1.0327	1.0319	1.0316
39	696.2	0.9991	0.9971	0.9963	0.9960	1.0383	1.0363	1.0356	1.0355
172.3	131.3	1.0060	1.0039	1.0031	1.0028	1.0545	1.0524	1.0517	1.0514
9.598	2766	1.0441	1.0441	1.0440	1.0440	1.0284	1.0284	1.0283	1.0283
9.426	2807	1.0335	1.0335	1.0334	1.0334	1.0175	1.0175	1.0174	1.0174

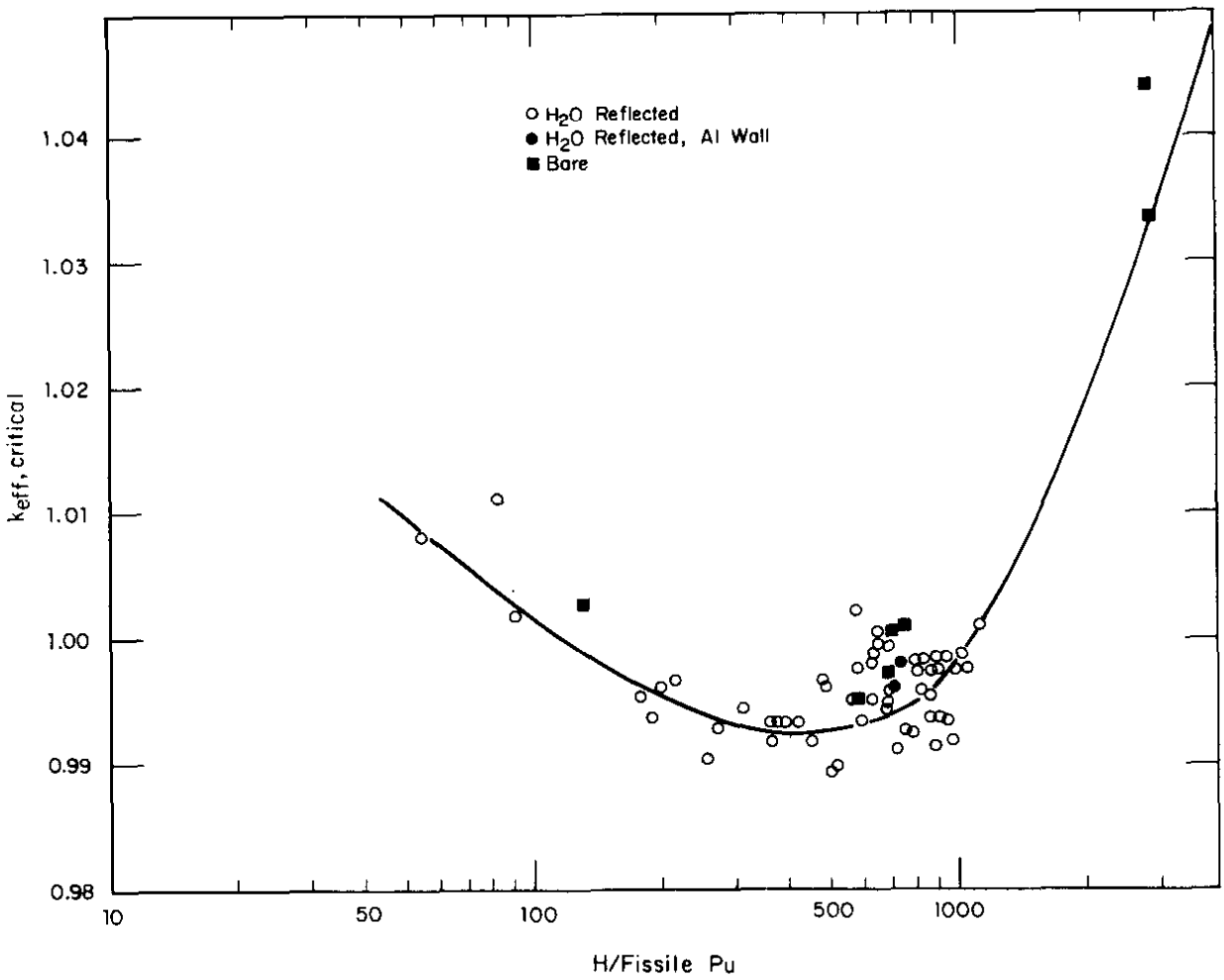

FIGURE 1. Correlation of HRXN-ANISN (S_∞) with $Pu(NO_3)_4$ Sphere Experiments

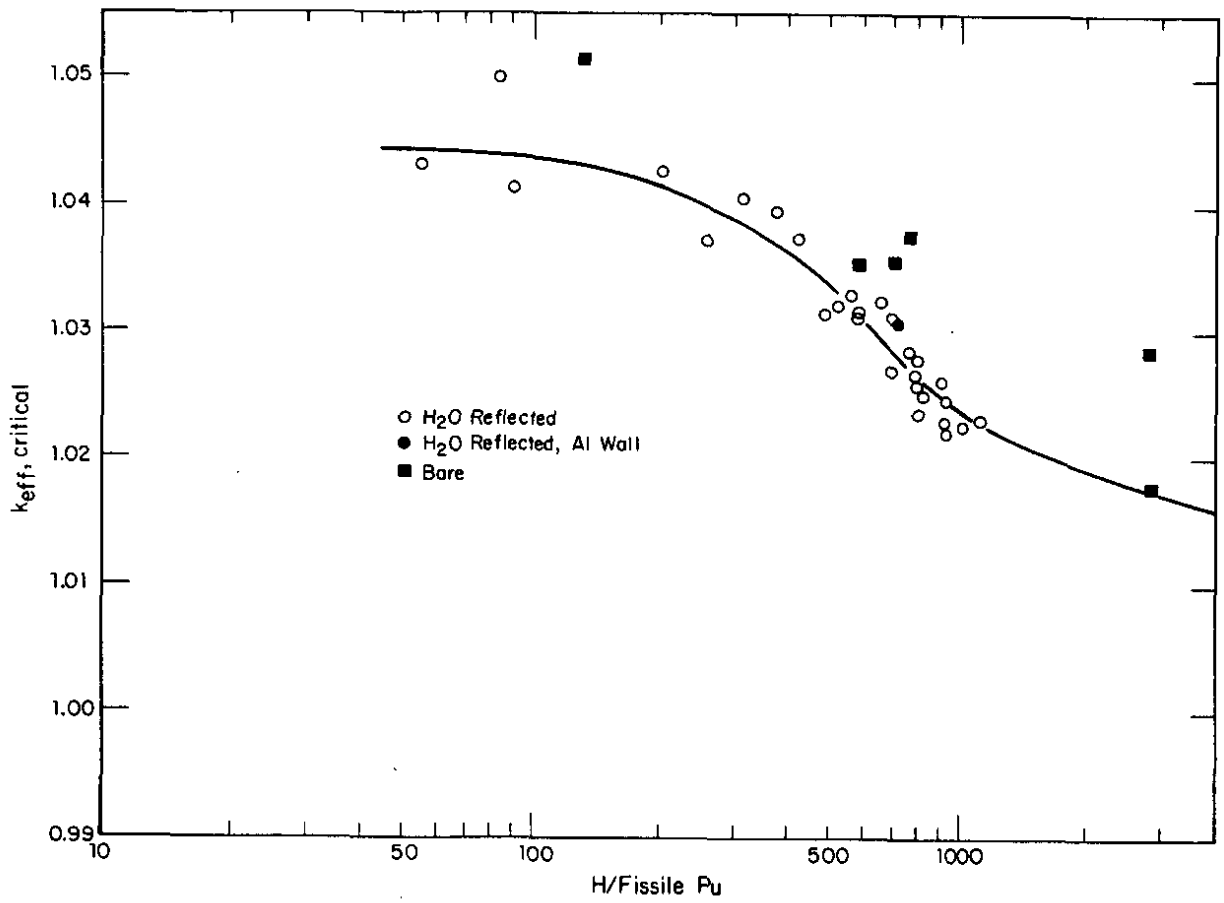

FIGURE 2. Correlation of GLASS-ANISN (S_∞) with $Pu(NO_3)_4$ Sphere Experiments

±0.0015, ±0.0013 to ±0.0039. The effect on k_{eff} was greatest for the highest nitrate and plutonium-240 concentrations, the bare sphere, and the lowest plutonium concentrations. Omitting the iron in solution from the P-11 Project experiments increased k_{eff} by only about 0.0001. Changing the composition of the steel shell to 2% manganese, 1% silicon, 11% nickel, 18% chromium, 68% iron reduced k_{eff} by 0.0006 for the reflected spheres and increased it by 0.0001 for the bare spheres. The mass error in the PNL experiments was reported to be ±1% except for the two high-concentration solutions where polymer and Pu(VI) were present where it was ±5.0%. The corresponding variations in k_{eff} ranged respectively, from ±0.0003 to ±0.0020 and from ±0.0009 to ±0.0015. Linear interpolation rather than a power fit to the data for the large sphere increased k_{eff} by 0.0014. For this sphere, an arbitrary 15% increase in nitrate concentration reduced k_{eff} by 0.0023.

Correlations with the sphere experiments were also made with MGBS-TGAN. The results are given in Table 14 in slightly different order from the listing of the experiments, but the experiments are identified by concentration and percent plutonium-240. The correlations with the P-11 Project experiments are a repetition of two earlier correlations[1,39] which differed from each other due to a change in the resonance treatment in MGBS and to including the sphere walls in the later calculations rather than correcting for them empirically. It was considered advisable to repeat the correlations, with apparent PuO_2 densities derived from the apparent molal volumes of Table 1 rather than the theoretical density (11.46 g/cm^3) used previously. The apparent densities are given in Table 14 as densities of $^{239}PuO_2$ (MGBS adjusts the density to the isotopic composition). No attempt was made to reduce solution density to correspond to a temperature greater than 20°C, as assumed by MGBS, by the introduction of voids. The small amount of iron present in the P-11 Project solutions was omitted since HRXN-ANISN calculations showed it to have an insignificant effect. The small differences in $H/^{239}Pu$ between Tables 13 and 14 result from the difference in temperature and, for the PNL experiments, the omission of plutonium-241 from the ratio calculated by MGBS. The critical k_{eff} in Table 14 is plotted in Figure 3 against H/Fissile plutonium.

A limited number of HRXN-KENO calculations were done for comparison with HRXN-ANISN results extrapolated to S_∞. Results are given in Table 15. The results from Table 13 are repeated and experiments are identified by concentration and sphere radius. A time limit of 5 minutes was specified for each case, and resulted in numbers of histories ranging from about 18,000 to 30,000.

TABLE 14

MGBS-TGAN Correlations with Sphere Experiments

^{240}Pu, %	Pu/ℓ, g	Apparent Density $^{239}PuO_2$, g/cm^3	$H/^{239}Pu$	k_{eff}
0.54	26.48	-44.25	980.8	0.9992
	26.50	-44.29	970.2	0.9940
	27.39	-45.22	928.6	0.9962
	28.28	-46.19	883.1	0.9945
1.76	33.55	-52.22	781.4	1.0028
	34.58	-53.56	750.3	1.0034
	35.57	-54.70	726.1	1.0027
	27.77	-45.33	936.5	0.9958
2.52	9.598	-31.09	2771.0	0.9961
	9.426	-30.99	2812.4	0.9856
3.12	135.8	72.50	185.3	>1.0213
	50.16	-86.36	520.4	1.0107
	51.74	-92.77	500.0	1.0106
	56.42	-111.8	451.1	1.0139
	59.97	-130.8	419.5	1.0157
	63.66	-160.1	390.0	1.0164
	70.44	-265.4	345.0	1.0172
	77.42	-729.7	308.8	1.0187
	36.25	-55.91	731.7	1.0086
	37.08	-57.24	707.4	1.0071
	37.70	-58.03	694.5	1.0069
	38.38	-59.38	675.9	1.0055
	40.92	-69.69	622.5	1.0077
	44.35	-71.84	560.1	1.0091
	28.81	-46.51	922.5	0.9984
	29.72	-47.57	886.8	1.0008
	30.16	-48.02	864.1	0.9983
	31.81	-50.00	799.9	0.9977
	35.55	-55.08	687.5	1.0011
	39.55	-61.38	591.6	1.0017
	24.97	-42.55	1053.7	0.9928
	25.73	-43.30	1011.4	0.9944
	27.15	-44.71	935.7	0.9952

TABLE 14 (Cont)

4.05	29.86	-47.75	898.6	0.9996
	30.73	-48.51	863.6	0.9999
	31.64	-49.62	830.5	1.0010
	33.76	-52.34	760.2	1.0024
	36.25	-55.84	691.1	1.0047
	38.71	-59.81	630.6	1.0049
	41.12	-64.02	580.7	1.0057
4.15	35.59	-54.94	749.7	1.0121
	38.13	-58.88	685.9	1.0138
	38.16	-59.28	681.1	1.0106
	43.43	-69.02	575.3	1.0118
4.40	30.80	-48.73	862.6	0.9966
	32.06	-50.21	819.3	0.9991
4.57	73	-312.1	370.8	1.0196
	74.5	-371.7	360.9	1.0183
	96	251.1	270.1	1.0197
	100	196.5	256.6	1.0175
	119	101.7	214.2	1.0229
	126	87.82	200.9	1.0222
	132	79.10	190.2	1.0207
	140	70.35	179.1	1.0220
	269	34.09	90.1	1.0232
	295	32.08	83.5	1.0308
	435	26.27	54.4	1.0264
	33.0	-50.83	798.9	1.0010
	33.2	-51.09	793.5	1.0018
	38.4	-58.44	652.9	1.0056
	38.6	-58.76	649.5	1.0065
	39.2	-59.73	634.1	1.0053
	47.5	-76.63	488.7	1.0066
	47.9	-77.65	483.8	1.0072
	24.4	-41.68	1120.5	0.9943
	38.7	-58.92	582.6	1.0048
	39.0	-59.40	699.7	1.0127
	172.3	51.20	132.3	1.0380

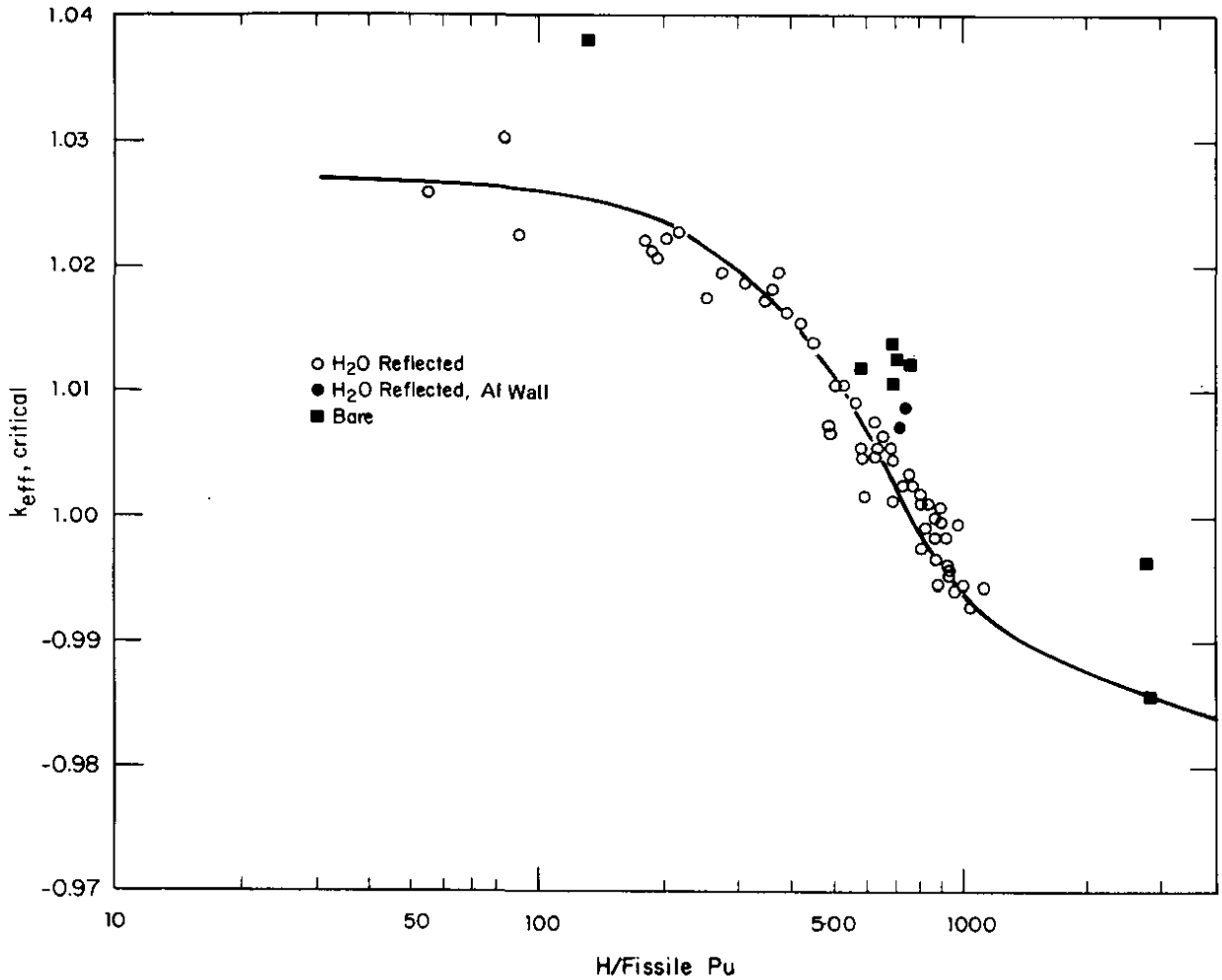

FIGURE 3. Correlation of MGBS-TGAN with $Pu(NO_3)_4$ Sphere Experiments

TABLE 15

HRXN-KENO Correlation with Selected Sphere Experiments

Conc Pu/ℓ, g	Sphere Radius, cm	k_{eff} HRXN-ANISN, S_∞	HRXN-KENO, Proposed Correction Absent	HRXN-KENO, Proposed Correction Present
135.8	13.95	>0.9906	>0.9911 ± 0.0053	>1.0038 ± 0.0057
59.97	15.36	0.9933	0.9750 ± 0.0054	1.0031 ± 0.0055
37.70	16.54	0.9958	0.9792 ± 0.0051	1.0056 ± 0.0061
39.55	17.80	0.9933	0.9901 ± 0.0060	1.0093 ± 0.0058
25.73	19.06	0.9987	1.0022 ± 0.0052	1.0015 ± 0.0057
35.59	20.13	1.0010	0.9972 ± 0.0049	1.0065 ± 0.0044
295.00	14.55	1.0113	1.0101 ± 0.0053	1.0080 ± 0.0059
47.5	17.67	0.9962	0.9932 ± 0.0058	1.0032 ± 0.0052
24.4	19.29	1.0010	0.9855 ± 0.0061	1.0079 ± 0.0051
172.3	19.45	1.0028	1.0017 ± 0.0053	1.0091 ± 0.0061

$Pu(NO_3)_4$ Solution Slabs

Values of k_{eff} calculated for the critical infinite slabs of Table 6 by HRXN-ANISN and by GLASS-ANISN are given in Table 16. Values calculated by MGBS-TGAN are given in Table 17. The order of listing is the same as in Table 6. Only S_{16} calculations were done by HRXN-ANISN. The variation of k_{eff} with quadrature should, however, be approximately that found with GLASS-ANISN. The uncertainty in k_{eff} associated with the experimental uncertainty of ±0.2 cm was investigated with HRXN-ANISN by increasing the slab thicknesses 0.2 cm and should be about the same with the other methods. The variations in the magnitudes of the differences obtained for bare and reflected slabs by the different methods are surprising. However, the reflected slab results are more directly pertinent to the calculation of limits since reflection is usually assumed. It is instructive to plot the biases of Tables 16 and 17 on the appropriate graph (Figures 1-3). There appears to be no reason to expect bias obtained from sphere experiments not to be appropriate for slabs. The high concentration of plutonium-240 in most of the experiments, however, causes deviation from the sphere curves. For HRXN-ANISN all the points at high plutonium-240 concentration lie above the curve; therefore, the curve is conservative for plutonium-240 concentrations above those (<5%) of the curve. For GLASS-ANISN, points fall on either side of the curve, but trend toward falling below it, particularly for reflected systems, at low H/Fissile plutonium. For MGBS-TGAN, there is a similar trend for H/Fissile plutonium less than about 200. Adequate allowance must be made for these trends in deriving subcritical limits.

$Pu(NO_3)_4$ Solution Cylinders

Consideration was given with HRXN-ANISN (S_{16}) to the P-11 Project cylinders of Table 3 to test the validity of applying bias established for spheres to the calculation of limits for infinite cylinders. Table 18 lists the experiments in the same order as Table 3. Values of k_{eff} for infinite slabs and infinite cylinders having dimensions of the finite cylinders are given. From these, axial and radial bucklings were derived by SPBL that when combined yielded the k_{eff} of the finite cylinders. Given also is the expected value of k_{eff} read from Figure 1 (ignoring the small difference between S_∞ and S_{16}). It appears that this method of treating finite bodies overestimates k_{eff}. When the overestimate is plotted against axial buckling, there is considerable scatter, but a linear relation going to zero at zero axial buckling does not appear unreasonable (a least squares fit to the data gives $\Delta k_{eff} = 0.0278$ at $B_z^2 = 0.01\ cm^{-2}$); hence, Figures 1 and 2 should be applicable to infinite cylinders. Some calculations were also made with HRXN-KENO.

TABLE 16

Correlation of HRXN-ANISN and GLASS-ANISN with $Pu(NO_3)_4$ Slab Experiments

		k_{eff}				
		HRXN-ANISN	*GLASS-ANISN*			
H/Fissile Pu	*Reflector*	S_{16}	S_4	S_8	S_{16}	S_∞
446	None	0.9996 ± 0.0085	1.0381	1.0438	1.0448	1.0451
	H_2O	1.0090 ± 0.0087	1.0299	1.0321	1.0322	1.0322
411	None	0.9995 ± 0.0078	1.0365	1.0416	1.0426	1.0429
	H_2O	0.9948 ± 0.0081	1.0236	1.0255	1.0256	1.0256
458	None	1.0152 ± 0.0060	1.0385	1.0424	1.0430	1.0431
	H_2O	1.0074 ± 0.0063	1.0257	1.0272	1.0273	1.0273
179	None	1.0162 ± 0.0057	1.0408	1.0446	1.0453	1.0455
	H_2O	1.0258 ± 0.0057	1.0438	1.0452	1.0453	1.0453
110.5	None	1.0199 ± 0.0050	1.0403	1.0437	1.0443	1.0445
	H_2O	1.0194 ± 0.0051	1.0336	1.0349	1.0349	1.0349
57.5	H_2O	1.0265 ± 0.0043	1.0335	1.0346	1.0346	1.0346
153	None	1.0168 ± 0.0049	1.0347	1.0380	1.0386	1.0388
	H_2O	1.0149 ± 0.0050	1.0279	1.0292	1.0293	1.0293
102.4	H_2O	1.0141 ± 0.0044	1.0225	1.0236	1.0237	1.0237

TABLE 17

Correlation of MGBS - TGAN with $Pu(NO_3)_4$ Slab Experiments

		k_{eff}	
H/Fissile Pu	*Apparent $^{239}PuO_2$ Density, g/cm^3*	*Bare*	*H_2O Reflected*
447.9	-114.4	1.0230	1.0242
413.2	-114.4	1.0184	1.0152
458.6	-183.0	1.0187	1.0171
179.1	56.39	1.0224	1.0290
110.7	36.85	1.0184	1.0160
57.4	26.68		0.9994
153.4	42.90	1.0140	1.0143
102.6	32.85		1.0058

TABLE 18

HRXN-ANISN Correlation with P-11 Project Cylinders

	k_{eff}					
					KENO, Proposed Correction	
$H/^{239}Pu$	*Infinite Slab*	*Infinite Cylinder*	*Finite Cylinder*	*Expected*	*Absent*	*Present*
333.3	1.5955	1.0238	>0.9748	0.9928		
234.8	1.5030	1.1173	1.0102	0.9943	0.9861 ± 0.0053	0.9896 ± 0.0053
261.6	1.5107	1.1163	1.0130	0.9937		
303.0	1.5142	1.1026	1.0059	0.9931		
352.5	1.5307	1.0945	1.0092	0.9927		
422.5	1.5409	1.0735	1.0021	0.9925	0.9911 ± 0.0056	0.9930 ± 0.0059
479.0	1.5509	1.0611	1.0004	0.9926		
333.3	1.4335	1.1550	1.0099	0.9928	0.9761 ± 0.0048	0.9799 ± 0.0057
335.4	1.4265	1.1541	1.0055	0.9928		
414.1	1.4385	1.1341	1.0023	0.9925		
526.1	1.4615	1.1040	1.0009	0.9927	0.9815 ± 0.0044	0.9759 ± 0.0056
663.8	1.4807	1.0667	0.9948	0.9936	0.9765 ± 0.0054	0.9907 ± 0.0058
408.2	1.3855	1.1936	1.0179	0.9925		
529.9	1.3918	1.1565	1.0064	0.9928		
553.8	1.4040	1.1556	1.0135	0.9929		
603.9	1.4216	1.1170	1.0060	0.9931		
663.8	1.4091	1.1197	1.0026	0.9936	0.9957 ± 0.0056	0.9996 ± 0.0058
659.7	1.4488	1.0770	1.0021	0.9935	0.9779 ± 0.0052	0.9923 ± 0.0057
774.1	1.4359	1.0895	1.0065	0.9948		
843.0	1.4506	1.0711	1.0077	0.9956		
234.8	1.3192	1.2738	1.0253	0.9943	0.9969 ± 0.0049	0.9947 ± 0.0059
536.9	1.3436	1.2063	1.0152	0.9928		
616.6	1.3603	1.1817	1.0173	0.9932		
719.1	1.3732	1.1582	1.0182	0.9941		
841.2	1.3809	1.1231	1.0116	0.9956		
983.2	1.3980	1.0798	1.0072	0.9980		

Correlations were made with the experiments with bare-topped cylinders. Both the separable treatment, involving ANISN and SPBL, and KENO were used. The KENO calculations gave a better representation of the experimental conditions in that the water reflector extended to the top of the vessel, which had a steel cover. Adjoint biasing was applied in the reflector which surrounded sides and bottom. In the ANISN calculations the top was simply bare. To force the mesh assignment scheme to treat the bulk of the plutonium solution as an intermediate region, the solution was subdivided into a thin upper layer and the remainder. Particularly for the large diameter cylinder used in the high burnup experiments, where solution heights were also fairly large, differences between extrapolation distances for finite and infinite vessels should have less effect than for small vessels, and the SPBL treatment should not introduce much, if any, nonconservatism. (Axial bucklings ranged from 0.001 to 0.003 so that, on the basis of the least squares fit to the P-11 Project cylinder data, Δk_{eff} associated with the separability treatment would be between 0.003 and 0.009). The correlations, listed in the same order as in Table 7 and recorded in Table 19, seem to bear this out when SPBL and KENO are compared.* As concluded from the slab experiments, applying the bias of Figure 1 to the calculation of subcritical limits by HRXN-ANISN for high concentrations of plutonium-240 appears quite conservative, but applying the bias of Figure 2 to the same calculation by GLASS-ANISN appears slightly nonconservative and adequate allowance for bias and uncertainty must be made.

PuO_2 Compacts

Correlations with the critical experiments with PuO_2 compacts described in Tables 8 through 11 are given, respectively, in Tables 20 through 23. The methods used were HRXN-ANISN and GLASS-ANISN, supplemented by KENO for some of the later experiments. The quadrature in ANISN was S_{16}. (The small difference between S_{16} and S_∞ in cases studied so far is hardly worth consideration, and certainly is not for the compacts in view of the large error flags).

Correlations with the experiments at H/Pu = 15 are given in Table 20. The uncertainties in k_{eff} correspond to reported dimensional uncertainties. No calculations were made for the bare, nearly cubic assemblies for which, in conjunction with

*It was not realized when these correlations were made that the top and bottom were 0.95 cm thick; 0.079 cm was assumed. ANISN calculations were repeated, but not KENO. Both sets of ANISN calculations are given in Table 19.

TABLE 19

Correlation with Cylinders with Bare Tops

H/Fissile Pu	k_{eff} HRXN-ANISN (S_{16})[a]	KENO[b]	GLASS-ANISN (S_{16})[a]	KENO[b]
85.5	1.0198	1.0070 ± 0.0053	1.0568	1.0314 ± 0.0050
	1.0138	1.0093 ± 0.0053	1.0479	1.0436 ± 0.0047
228.4	1.0127	1.0040 ± 0.0054	1.0625	1.0428 ± 0.0054
	0.9871	1.0155 ± 0.0049	1.0320	1.0592 ± 0.0057
301.4	1.0275	1.0254 ± 0.0037	1.0233	1.0227 ± 0.0041
	1.0257	1.0276 ± 0.0039	1.0195	1.0282 ± 0.0038
378.4	1.0323	1.0296 ± 0.0042	1.0283	1.0274 ± 0.0037
	1.0302	1.0354 ± 0.0042	1.0239	1.0231 ± 0.0039
451.5	1.0319	1.0285 ± 0.0039	1.0277	1.0160 ± 0.0040
	1.0295	1.0183 ± 0.0039	1.0230	1.0262 ± 0.0041
535.5	1.0312	1.0292 ± 0.0036	1.0264	1.0174 ± 0.0035
	1.0288	1.0310 ± 0.0041	1.0214	1.0288 ± 0.0035
614.2	1.0309	1.0195 ± 0.0042	1.0250	1.0071 ± 0.0040
	1.0285	1.0251 ± 0.0034	1.0202	1.0147 ± 0.0041
722.5	1.0299	1.0205 ± 0.0037	1.0226	1.0171 ± 0.0038
	1.0278	1.0263 ± 0.0036	1.0181	1.0160 ± 0.0038
845.8	1.0294	o.0317 ± 0.0035	1.0202	1.0166 ± 0.0036
	1.0276	1.0263 ± 0.0036	1.0163	1.0149 ± 0.0036
1030	1.0293	1.0220 ± 0.0034	1.0169	1.0055 ± 0.0029
	1.0282	1.0259 ± 0.0033	1.0141	1.0215 ± 0.0035
1196	1.0279	1.0271 ± 0.0031	1.0129	1.0113 ± 0.0027
	1.0273	1.0270 ± 0.0032	1.0110	1.0143 ± 0.0030

a. First result obtained with 0.079-cm-thick bottom; second result with correct thickness, 0.95 cm.

b. First result obtained without proposed change in KENO, second with it. Both sets made with 0.079 cm thickness for top and bottom.

TABLE 20

Correlation with Infinite Bare and Plexiglas Reflected Slabs at H/Pu = 15

H/Fissile Pu	*Reflector*	*Particle Size Correction*	k_{eff} *HRXN-ANISN*	*GLASS-ANISN*
15.42	None	No	1.0286 ± 0.0195	1.0738 ± 0.0187
		Yes	1.0224 ± 0.0257	1.0679 ± 0.0246
	Plexiglas	No	1.0425 ± 0.0050	1.0615 ± 0.0049
		Yes	1.0445 ± 0.0070	1.0635 ± 0.0069
16.27	None	No	1.0012 ± 0.0149	1.0459 ± 0.0143
		Yes	1.0106 ± 0.0243	1.0540 ± 0.0234
	Plexiglas	No	1.0240 ± 0.0034	1.0418 ± 0.0034
		Yes	1.0315 ± 0.0109	1.0494 ± 0.0110

TABLE 21

Correlation with Infinite Bare and Reflected Slabs at H/Pu = 5 (H/Fissile Pu = 5.70)

Reflector	*Extrapolation Method*	k_{eff} *HRXN-ANISN*	*GLASS-ANISN*
None	λ^a	1.0431 ± 0.0138	1.1346 ± 0.0142
Plexiglas	λ^b	1.0361 ± 0.0050	1.0910 ± 0.0054
	Critical height[c]	1.0311 ± 0.0105	1.0857 ± 0.0113

a. Based on calculated difference in extrapolation distance for a cube and an infinite slab.

b. Extrapolation of effective extrapolation distance as a function of transverse buckling.

c. Extrapolation of critical height as a function of inverse cross-sectional area.

TABLE 22

Correlation with Critical Experiments with PuO_2 Compacts

A. Reflected Cuboids

Height, cm	k_{eff} HRXN-ANISN-SPBL	k_{eff} KENO[a]	k_{eff} GLASS-ANISN-SPBL	k_{eff} KENO[a]
10.03	1.1256	1.0199 ± 0.0055	1.1151	1.0647 ± 0.0077
		1.0350 ± 0.0048		1.0827 ± 0.0077
8.98	1.1201	1.0319 ± 0.0061	1.1118	1.0688 ± 0.0067
		1.0267 ± 0.0066		1.0805 ± 0.0069
7.97	1.1107	1.0268 ± 0.0063	1.1053	1.0591 ± 0.0067
		1.0282 ± 0.0067		1.0727 ± 0.0070
6.86	1.0970	1.0187 ± 0.0070	1.0960	1.0618 ± 0.0066
		1.0178 ± 0.0069		1.0825 ± 0.0079
5.95	1.0837	1.0090 ± 0.0070	1.0874	1.0652 ± 0.0076

a. First result obtained without proposed correction to KENO, second, with it.

B. Infinite Slabs

Reflector	Extrapolation Method	k_{eff} HRXN-ANISN	k_{eff} GLASS-ANISN
None	λ[a]	1.0485 ± 0.0184	1.0252 ± 0.0182
Plexiglas	λ[b]	0.9921 ± 0.0409	1.0212 ± 0.0380
	Critical height[c]	1.0228 ± 0.0093	1.0497 ± 0.0086
	k_{eff}[d]	1.0335	1.0536

a. Based on calculated difference in extrapolation distance for a cube and an infinite slab.

b. Extrapolation of effective extrapolation distance as a function of inverse cross-sectional area.

c. Extrapolation of critical height as a function of inverse cross-sectional area.

d. Least squares linear extrapolation of SPBL k_{eff} as function of transverse buckling.

TABLE 23

Correlation with Critical Experiments with Compacts at H/Pu = 50 (H/Fissile Pu = 62.3)

A. Reflected Cuboids

	k_{eff}			
	HRXN-		*GLASS-*	
Height, cm	*ANISN-SPBL*	*KENO*[a]	*ANISN-SPBL*	*KENO*[a]
29.64	1.0361	1.0095 ± 0.0053	1.0429	1.0051 ± 0.0060
		1.0175 ± 0.0060		1.0160 ± 0.0051
23.58	1.0347	1.0033 ± 0.0055	1.0415	1.0076 ± 0.0055
		1.0119 ± 0.0064		1.0030 ± 0.0055
22.06	1.0342	1.0090 ± 0.0062	1.0415	1.0042 ± 0.0059
		1.0266 ± 0.0057		1.0124 ± 0.0055
19.69	1.0328	1.0083 ± 0.0065	1.0394	1.0022 ± 0.0054
		1.0101 ± 0.0061		1.0045 ± 0.0056
18.68	1.0311	1.0155 ± 0.0065	1.0376	1.0123 ± 0.0050
		1.0170 ± 0.0057		1.0141 ± 0.0054
17.48	1.0301	1.0108 ± 0.0053	1.0365	1.0047 ± 0.0051
		1.0143 ± 0.0065		1.0057 ± 0.0054
16.35	1.0285	0.9945 ± 0.0060	1.0347	1.0004 ± 0.0054
		1.0027 ± 0.0062		1.0079 ± 0.0064

a. First result obtained without proposed correction to KENO, second, with it.

B. Infinite Slabs

		k_{eff}	
Reflector	*Extrapolation Method*	*HRXN-ANISN*	*GLASS-ANISN*
None	λ[a]	1.0214 ± 0.0063	1.0337 ± 0.0059
Plexiglas	λ[b]	1.0156 ± 0.0048	1.0199 ± 0.0046
	Critical height[c]	1.0110 ± 0.0034	1.0155 ± 0.0032
	k_{eff}[d]	1.0229	1.0287

a. Based on calculated difference in extrapolation distance for a cube and an infinite slab.

b. Extrapolation of effective extrapolation distance as a function of inverse cross-sectional area.

c. Extrapolation of critical height as a function of inverse cross-sectional area.

d. Least squares linear extrapolation of SPBL k_{eff} as function of transverse buckling.

calculated extrapolation distances, bucklings were derived by the experimenters to be used in the analysis of the reflected assemblies. The critical bucklings at 2.2% and 8% plutonium-240 were, respectively, 0.02227 and 0.01733 cm^{-2}. These may be compared with critical bucklings of 0.023128 and 0.016837 cm^{-2} calculated by HRXN and with bucklings of 0.025856 and 0.018981 cm^{-2} from GLASS cross sections. The Plexiglas™ reflector group constants were weighted by the plutonium fission spectrum. In some calculations, however, the uranium-235 spectrum from the Standard Library was inadvertently used, increasing k_{eff} by about 0.0007.

Correlations with the experiments at H/Pu = 5 are given in Table 21. Calculations made for the bare cuboid with the SPBL technique gave 1.0526 by HRXN-ANISN, 1.1470 by GLASS-ANISN, in reasonable agreement with the infinite slab results, when account is taken of the approximation in SPBL. The buckling derived by the experimenters from the cuboid dimensions and a calculated bare extrapolation distance was 0.01945 cm^{-2}. Those calculated by HRXN and GLASS were, respectively, 0.020463 and 0.02502 cm^{-2}. In some GLASS calculations, carbon cross sections from the Standard Library rather than those processed from ENDF/B-III were inadvertently used, increasing k_{eff} about 0.0010.

Correlations with the experiments with dry PuO_2 are given in Table 22. Calculations for the bare cuboid by the SPBL technique gave 1.0941 $\pm$0.0044 by HRXN-ANISN, 1.0704 $\pm$0.0044 by GLASS-ANISN, substantially above the infinite slab results and above HRXN- and GLASS-KENO results for the cuboid: 1.0321 $\pm$0.0043 and 1.0119 $\pm$0.0045 without the proposed correction to KENO, 1.0326 $\pm$0.0048 and 1.0327 $\pm$0.0052 with it. (The SPBL uncertainty corresponds to the reported dimensional uncertainty; the KENO uncertainty is one standard deviation.) The critical buckling derived by the experimenters from the cuboid dimensions and a calculated bare extrapolation distance was 0.02620 cm^{-2}. Those calculated by HRXN and GLASS were 0.028825 and 0.028517 cm^{-2}, respectively. Extrapolation to the reflected slab is somewhat uncertain, but the critical height and k_{eff} extrapolation give the best agreement with the Monte Carlo results. (Adjoint biasing was used in the reflector with weights furnished with KENO for paraffin.) It is worth noting that despite similarities in critical bucklings and migration areas calculated by HRXN and GLASS, k_{eff}'s are appreciably different and the difference reverses sign for reflected assemblies compared to bare assemblies. In the Glass calculations, the combined spectrum treatment was used to generate the cross sections for the oxide.

Correlation with the experiments with polystyrene compacts at H/Pu = 50 are given in Table 23. Calculations for the bare cuboid

by the SPBL technique gave 1.0237 by HRXN-ANISN, 1.0358 by GLASS-ANISN, close to the infinite slab results but appreciably above HRXN- and GLASS-KENO results for the cuboid: 1.0121 ±0.0047 and 1.0026 ±0.0049 without the proposed corrections, 1.0119 ±0.0047 and 1.0159 ±0.0047 with it. The critical buckling derived by the experimenters from the cuboid dimensions and a calculated bare extrapolation distance was 0.01162 cm^{-2}. Those calculated by HRXN and GLASS were 0.01206 and 0.01270 cm^{-2}, respectively. Extrapolation to the infinite slab thickness is less uncertain than for dry oxide. SPBL k_{eff} as a function of transverse buckling is fitted better by a quadratic than by a linear expression. Extrapolation of least squares quadratic fits gives HRXN- and GLASS-ANISN values of k_{eff} of 1.0131 and 1.0162 for the infinite slab, in better agreement with the other two methods.

Plutonium Metal

Correlations with the three metal sphere experiments of Table 13 are given in Table 24. The HRXN-ANISN results are a repeat of previous work.[40] Why they differ by as much as 0.0003 in k_{eff} is not known since input should have been identical. The uncertainty in k_{eff} associated with experimental uncertainties ranges from ±0.0012 to ±0.0022. The two bare sphere correlations were made to see how well GLASS-ANISN handles plutonium-240 in metal systems. Gallium was replaced by nickel, since there are no cross sections for gallium in the GLASS libraries.

TABLE 24

Correlation with Pu Metal Spheres

		k_{eff}							
		HRXN-ANISN				GLASS-ANISN			
Reflector	^{240}Pu, %	S_4	S_8	S_{16}	S_∞	S_4	S_8	S_{16}	S_∞
None	4.5	1.0158	1.0059	1.0029	1.0018	1.0103	1.0005	0.9976	0.9965
	20.1	1.0220	1.0123	1.0093	1.0082	1.0082	0.9987	0.9958	0.9947
Water	5.18	1.0156	1.0006	0.9965	0.9951	1.0262	1.0117	1.0077	1.0063

SUBCRITICAL LIMITS

The American National Standard for Nuclear Criticality Safety in Operations with Fissionable Materials Outside Reactors (ANS-8.1/ ANSI N16.1-1975) is due for its quinquennial review. As part of the review, limits presently in the Standard are being examined, and it seems worthwhile to extend them. In the case of plutonium nitrate solutions and PuO_2 slurries, an extension to 5% plutonium-240, 0.5% plutonium-241, and to the isotopic compositions of the recently issued Standard, "Nuclear Criticality Control and Safety of Homogeneous Plutonium-Uranium Fuel Mixtures Outside Reactors," ANSI/ ANS-8.12-1978, namely 15% plutonium-240, 6% plutonium-241, and 25% plutonium-240, 15% plutonium-241, should prove useful. The addition of limits for PuO_2 to those now provided for metal should also prove useful. The limits in the Standard apply to units surrounded by materials (including other units) no more effective in returning neutrons than a contiguous reflector of water of unlimited thickness and are "maximum" subcritical limits. The limiting masses, dimensions, and concentrations are intended to be subcritical under the stated conditions, but also sufficiently close to critical to discourage attempts to justify larger limits. The mass and concentration limits are not appropriate for operating limits, since they contain no allowance for operating errors, such as double batching, or for uncertainties as to precise values of process variables. Similarly, the dimensional limits contain no allowance for tolerances in the construction of vessels, for bulging of vessels, or for corrosion.

The limits for $Pu(NO_3)_4$ solution apply only to uniform aqueous solutions. They take no credit for nitric acid; therefore, in practice, the limits would generally have a margin of subcriticality additional to that allowed in the calculations since in order to prevent polymerization and precipitation of the plutonium and hence to maintain a uniform solution, it is necessary to have a nitric acid concentration of about 1.5M.[11] However, it would be improper to count on this in deriving the limits. The user of the Standard has the right to expect that the limiting values would actually be subcritical under the stated conditions. It should be legitimate for him, if he so chooses, to use the limits as points of departure in arriving at larger limits by taking credit for nitric acid, finite cylinder heights, less effective reflectors, etc., provided the extensions are made conservatively.

All three methods, HRXN-ANISN, GLASS-ANISN, and MGBS-TGAN, were used for the calculation of limits for $Pu(NO_3)_4$ solutions. The S_n quadrature was S_{16}, the small difference between S_∞ and S_{16} being ignored. MGBS-TGAN was used partly because of its extended use in the past, including its use to generate limits for the mixed oxide Standard.[40] Where the methods disagree, one might be inclined to give greatest credence to GLASS-ANISN with its cross sections derived from ENDF/B-IV, including cross sections for H

in the lower groups conforming to a thermal scattering law for H_2O, its direct use of resonance parameters by way of the Nordheim integral treatment (although something seems amiss in the resonance treatment since at very high concentrations of fissile nuclides resonance reaction rates exceed source rates from slowing down), and its use of S_n transport theory in 16 groups for performing the reactor calculation. However, the older, more approximate method MGBS-TGAN[1,39] cannot be dismissed out of hand as being overly conservative. GLASS cross sections collapsed to 2 groups rather than 16 and adjusted for the difference in leakage expressions between diffusion theory and transport theory (as in MGBS) gave for uranium-235 solutions close to the same bias in GLASS-TGAN calculations as was obtained in 16 group GLASS-ANISN calculations, especially at the lower concentrations; hence, two-group diffusion theory is not grossly inadequate. The resonance integrals in MGBS are tabulated as a function of potential scattering cross section per atom of absorber with especial care not to include plutonium-240 contributions below the thermal energy cutoff. The nitrogen, hydrogen, and oxygen cross sections in the epithermal groups are a function of nitrate concentration and were determined at N/H ratios of 0, 0.04, and 0.08 in infinite medium, zero buckling slowing down calculations, from a fission source, with lethargy width 0.1. The thermal group cross sections have been averaged over 110 groups, rather than 29 as in GLASS, albeit having been calculated with the Wigner-Wilkins gas kernel rather than a thermal scattering law for H_2O[7]. The bias of GLASS-ANISN is larger than that of MGBS-TGAN, but the latter shows more variation with H/Pu.

Minimum critical parameters calculated by the three methods for water-reflected aqueous solutions of $Pu(NO_3)_4$ at 20°C with 100% plutonium-239, as in the Standard, are given in Table 25. The minima were determined from graphical plots of the parameter of interest as a function of concentration. The plotted parameters are those calculated to correspond to critical values of k_{eff} read from Figures 1-3. (An example showing the derivation of minimum critical mass is given in Appendix B.) The MGBS-TGAN results for mass, cylinder diameter, and slab thickness are approximately equal to the subcritical limits in the Standard. Included in Table 25 are results obtained by Richey,[13,41], whose calculations served as the basis for limits in the Standard. His method was 18-group diffision theory, with thermal group constants averaged over a Wigner-Wilkins spectrum and epithermal group constants derived from a 64 group B_1 calculation, and agreed well with experiments, with essentially no bias. The disagreement among methods all normalized to the same experimental data is somewhat surprising, particularly in the case of mass since many experiments were performed in the concentration range where minimum mass occur. The spread in values corresponds to about 2% in k_{eff}.

TABLE 25

Minimum Critical Parameters of Aqueous Solutions of $Pu(NO_3)_4$ with 100% ^{239}Pu

Parameter	*HRXN-ANISN*	*GLASS-ANISN*	*MGBS-TGAN*	*Richey*
Mass Pu, kg	0.535	0.526	0.510	0.547
Cylinder Dia., cm	16.12	15.96	15.74	16.30
Slab Thickness, cm	5.94	6.02	5.76	6.21
Volume, ℓ	8.22	7.89	7.81	8.32
Conc., g Pu/ℓ	7.62	7.58	7.46	
H/Pu	3475	3490	3546	
Areal Density, g Pu/cm^2	0.268	0.272	0.262	

A careful study of each method would be necessary in order to discover the sources of the discrepancies. There may be trends in the bias as a function of nitrate and plutonium-240 concentration that are not readily apparent. Richey's use of a density formula in his parametric survey calculations as opposed to his use of analytical data in correlating with experiments may have introduced some error. The treatment of the stainless steel vessel wall may introduce some error. Back calculation of two reflected sphere experiments with the critical values of k_{eff} determined in correlations were made with and without the steel walls. With the walls present, experimental conditions were reproduced satisfactorily, demonstrating the correctness of the radius search corresponding to a specified value of k_{eff}. Without the walls, MGBS-TGAN gave the lowest masses, indicating it calculates the greatest effect. HRXN-ANISN was next. Differences were small, however, slightly less than 1% in mass between GLASS-ANISN and MGBS-TGAN.

Calculations were extended to the minimum critical mass of water-reflected uniform, homogeneous PuO_2-H_2O mixtures. HRXN-ANISN, GLASS-ANISN, and MGBS-TGAN yielded, 525, 512, and 496 g plutonium respectively. Richey's value was 531 g. At the low concentration at which the mimimum mass occurs, it makes little difference whether the mixture is Pu-H_2O, Pu_2O_3-H_2O, or a fictitious PuO_2F_2-H_2O for which other calculations have been made. A semiempirical analysis of the P-11 Project data led to a minimum critical mass of 506 g.[42] An analysis of the data with an earlier version of MGBS-TGAN[39] having a slightly different resonance treatment[1] and with an empirical correction made for the vessel walls resulted in very little bias. Calculated bucklings, after allowance for slight changes in cross sections to conform to those used in the data analysis but without allowance for bias, led to a minimum critical mass of 498 g plutonium. Subsequent use of this analysis with the bias expressed as a function of concentration led to a minimum critical mass of 512 g.[43] In a compendium of critical mass data, the minimum of the mass versus concentration curve is about 510 g.[44] The experimenters in the P-11 Project concluded that the minimum critical mass was 509 g contained in the thin steel shell of the experiments.[24] Without the shell, the mass would be reduced to about 490 g.

It was thought that perhaps part of the reason for the discrepancy in the results obtained by the three methods of calculation might lie in differences in the "eyeball" fits to the data in Figures 1-3. Accordingly, the critical mass calculations for $Pu(NO_3)_4$ and PuO_2 were normalized to the experiment with plutonium containing 0.54% plutonium-240 at 27.39 g Pu/ℓ. For 0.12M plutonium [H/Pu = 915.2 for $Pu(NO_3)_4$, 920.9 for PuO_2] the critical masses calculated by HRXN-ANISN, GLASS-ANISN, and MGBS-TGAN normalized to the curves in Figures 1-3 were, respectively, for $Pu(NO_3)_4$, 539, 529, and 515 g and for PuO_2, 528, 517, and 501 g plutonium. Normalized to the single experiment, the respective results were 532, 525, and 517; 522, 513, and 503. Thus, the normalization is partly responsible for the discrepancy.

The selection of limits is necessarily somewhat arbitrary. Those presently in the Standard for mass, cylinder diameter, slab thickness, and volume of $Pu(NO_3)_4$ solutions are purportedly values calculated by Richey[13] to correspond to a k_{eff} of 0.98. However, the mass and volume limits in the Standard are slightly higher and were taken from his earlier paper.[41] From an examination of the scatter about the curves of Figures 1-3 and from the experimental uncertainties expressed in terms of variation in k_{eff} it would appear that a margin in k_{eff} of 0.01 should be sufficient to assure subcriticality, i.e., that conditions corresponding to k_{eff} = 1 + Bias - 0.01 should be subcritical. The conditions for which the limits are given represent some extension of experimental conditions to 0% plutonium-240, zero nitric acid molarity, and zero vessel wall thickness, but there are no obvious variations in

the bias with these parameters. For good measure, however, it is desirable to assign an extra margin, say 0.01, making the total margin 0.02. However, with three (four including Richey's) methods, a margin this great applied to the most conservative, particularly when it may have the most approximations, appears excessive. On the other hand, unless a method can clearly be rejected, results calculated by a second method with margin 0.02, which the former method predicts would be critical, should not be accepted as limits. Thus, the limits in the Standard, which MGBS-TGAN predicts would be critical, are too large, even though Richey's method looks quite good.

Table 26 lists "limits" (i.e., parameters correponding to a margin in k_{eff} of 0.02) calculated by the four methods, together with limits now in the Standard and limits proposed for the revised standard. The margin in k_{eff} is not on the same basis for the two ANISN methods as for MGBS-TGAN. In the former methods, k_{eff} is number of neutrons produced per fission source neutron for a steady state solution. In TGAN, a fictitious transverse buckling increment is added to each region such that the core buckling results in the desired k_{eff} calculated as $k/(1 + M^2B^2)$. It is apparent by comparing Tables 25 and 26 that a margin of 0.02 in k_{eff} produces a larger change in a parameter in TGAN than it does in ANISN. The proposed limits are generally subcritical by a margin of about 0.01 relative to MGBS-TGAN critical values. The concentration limit in the Standard was reduced in the 1975 revision from its original value. The reduction was as a result of doubts[45] based on data then available, that the limit was subcritical and as the result of a re-examination of experimental data.[46]. The recent experiments in the large sphere[25] permit it to be raised to its former value. The slurry mass limit has been left at its former value although the margin of subcriticality may be smaller than that supposed.[43]

In Tables 27, 28, and 29, "limits" (again parameters corresponding to a margin of 0.02 relative to the curves of Figures 1-3) are calculated for $Pu(NO_3)_4$ solution in which the plutonium contains 5% plutonium-240, 0.5% plutonium-241; 15% plutonium-240, 6% plutonium-241; and 25% plutonium-240, 15% plutonium 241 by weight. In plutonium actually encountered, plutonium-238 and plutonium-242 will be present. However, it is conservative either to treat them as plutonium-239 or to omit them from the composition in computing the percentages of plutonium-240 and plutonium-241. Also given in the three tables are suggested limits for the revised Standard. The latter two compositions are those adopted for the mixed oxide Standard. The other composition was an intermediate one that seemed to offer some utility. The plutonium-241 concentration was selected on the basis of compositions in the experiments with which correlations were made. Increasing it to 1.5% plutonium-241 reduces the margin of subcriticality by only about 0.002, as calculated by MGBS-TGAN. This amount is fairly insignificant; therefore, the suggested limits should be valid up to 1.5% plutonium-241.

TABLE 26

Limits for Aqueous Systems Containing Plutonium
100% ^{239}Pu

Parameter	Standard	Source (Ref)	HRXN-ANISN	GLASS-ANISN	MGBS-TGAN	Revised Standard
A. Solutions of $Pu(NO_3)_4$						
Mass Pu, kg	0.51	0.499 (21)	0.489	0.477	0.453	0.480
Cylinder Dia., cm	15.7	15.68 (21)	15.58	15.42	15.02	15.4
Slab Thickness, cm	5.8	5.79 (21)	5.62	5.68	5.27	5.5
Volume, ℓ	7.7	7.53 (21)	7.55	7.24	6.97	7.3
Conc., g Pu/ℓ	7.0	7.0 (55, 56)	7.35	7.29	7.16	7.3
H/Pu			3600	3630	3700	3630
Areal Density, g Pu/cm^2	0.25	0.25 (53)	0.255	0.254	0.245	0.25
B. PuO_2 - H_2O Slurry						
Mass Pu, kg (Uniform Slurry)		∿0.470 (53)	0.478	0.466	0.444	
Mass Pu, kg (Non-uniform slurry)	0.450	0.450 (53)				0.450

TABLE 27

Limits for Aqueous Solutions of $Pu(NO_3)_4$ with ≥5% ^{240}Pu, ≤0.5% ^{241}Pu

Parameter	HRXN-ANISN	GLASS-ANISN	MGBS-TGAN	Revised Standard
Mass Pu, kg	0.580	0.576	0.549	0.570
Cylinder Dia., cm	17.38	17.53	17.19	17.4
Slab Thickness, cm	6.72	7.01	6.59	6.7
Volume, ℓ	10.03	10.07	9.88	10.0
Conc., g Pu/ℓ	7.89	7.84	7.70	7.8
H/Pu	3350	3373	3435	3400
Areal Density, g Pu/cm^2	0.282	0.283	0.272	0.28

TABLE 28

Limits for Aqueous Solution of Pu $(NO_3)_4$ with $\geq$15% ^{240}Pu, $\leq$6% ^{241}Pu

Parameter	*HRXN-ANISN*	*GLASS-ANISN*	*MGBS-TGAN*	*Revised Standard*
Mass Pu, kg	0.778	0.806	0.764	0.78
Cylinder Dia., cm	19.48	20.02	19.62	19.5
Slab Thickness, cm	8.02	8.55	8.05	8.0
Volume, ℓ	13.55	14.36	13.94	13.6
Conc., g Pu/ℓ	9.00	9.01	8.80	8.9
H/Pu	2937	2935	3005	2980
Areal Density, g Pu/cm^2	0.338	0.343	0.331	0.34

TABLE 29

Limits for Aqueous Solutions of Pu $(NO_3)_4$ with $\geq$25% ^{240}Pu, $\leq$15% ^{241}Pu

Parameter	*HRXN-ANISN*	*GLASS-ANISN*	*MGBS-TGAN*	*Revised Standard*
Mass Pu, kg	1.023	1.109	1.027	1.02
Cylinder Dia., cm	21.25	22.25	21.51	21.3
Slab Thickness, cm	9.11	9.91	9.24	9.2
Volume, ℓ	17.21	19.10	17.86	17.2
Conc., g Pu/ℓ	10.23	10.34	10.02	10.2
H/Pu	2587	2558	2640	2600
Areal Density, g Pu/cm^2	0.402	0.416	0.396	0.40

The curves in Figures 1 through 3 are appropriate for the 5% plutonium-240 composition; many of the experiments were with plutonium containing 4.6% plutonium-240. As pointed out earlier, the curve in Figure 1 appears conservative for plutonium containing 18 to 43% plutonium-240 as judged from the slab and large cylinder experiments. The curve in Figure 2 may be slightly nonconservative. That in Figure 3 appears appropriate for the higher plutonium-240 concentrations at H/Fissile plutonium >200. The range of H/Fissile plutonium within which the critical concentration, mass, and dimensional minima occur shrinks at both ends with increasing plutonium-240 concentration from 60 to 3500 at 0% plutonium-240 to 200 to 2500 at 25% plutonium-240; therefore, the curve in Figure 3 should not introduce appreciable nonconservatism into MGBS-TGAN calculations. The largest difference in limits occurs for 25% plutonium-240 and is in the expected direction. A margin from the curve of Figure 2 greater than 0.03 (rather than 0.02 as used in the calculation) would be required to bring the GLASS-ANISN results in line with the others.

Only MGBS-TGAN calculations were used to derive mass limits for PuO_2 slurries with plutonium-240 concentrations >5%. In view of the lack of any indication of nonconservatism in MGBS-TGAN and of the small increases in k_{eff} (0.007)[43] resulting from distributing the minimum critical mass in a uniform distribution optimally, it was concluded that masses calculated by MGBS-TGAN for uniform distributions with Δk_{eff} of 0.02, relative to the curve of Figure 3, would assuredly be subcritical for any nonuniform distribution. Masses of plutonium so calculated for 5%, 15%, and 25% plutonium-240 and 1.5%, 6%, and 15% plutonium-241 are 530, 740, and 990 g, respectively.

Besides the limits for aqueous systems, the general Standard contains limits for plutonium metal reflected by no better reflector than water. As indicated previously, it is desirable to examine these limits and to extend them to oxide. The two methods adopted for the calculations were HRXN-ANISN and GLASS-ANISN. For metal, the quadrature was extrapolated to S_∞, but for the oxide, S_{16} was adopted. As is apparent from Table 22, the bias for the oxide calculation has a large element of uncertainty. However, it appears that adopting the bias for a water-reflected sphere (Table 24) for both metal and oxide calculations should certainly be conservative for oxide. As in the solution calculations, a margin of 0.02 was allowed to assure subcriticality. Metal was assumed to have a density of 19.82 (Lange's Handbook) and oxide a density of 11.46 g/cm^3. The calculations were made for 100% plutonium-239, but they can be applied to any isotopic composition, provided plutonium-240 exceeds plutonium-241 (calculations for 50-50 plutonium-240 plutonium-241 gave a much higher critical mass than for plutonium-239). Although plutonium-238 may have a lower bare critical mass than plutonium-239, such is not the case with

water reflection. Calculations were made both for dry oxide and damp oxide (H/Pu = 0.45, 1.48% H_2O) as in the mixed oxide Standard, but limits were lower for dry oxide. However, as H/Pu increases, the mass must eventually drop; therefore, some limit on H/Pu is necessary and it might as well be that adopted for the mixed oxide Standard. The calculated limits are given in Table 30. For metal, the two methods agree with each other and with the limits presently in the Standard.

TABLE 30

Limits for Pu Metal and Oxide

Material	*Parameter*	*HRXN-ANISN*	*GLASS-ANISN*	*Standard*	*Revised Standard*
Metal	Mass Pu, kg	5.05	5.03	4.9	5.0
@19.82 g Pu/cm^3	Cyl. Dia., cm	4.39	4.38	4.4	4.4
	Slab Thickness, cm	0.70	0.63	0.65	0.65
Oxide@	Mass Pu, kg	11.06	10.17		10.2
11.46 g PuO_2/cm^3 (H/Pu <0.45)	Mass PuO_2, kg	12.54	11.53		11.5
	Cyl. Dia., cm	7.47	7.22		7.2
	Slab Thickness, cm	1.60	1.41		1.4
Oxide,@	Mass Pu, kg	29.93	27.00		27.0
5.78 g PuO_2/cm^3	Mass PuO_2 kg	33.94	30.62		30.6
(H/Pu <0.45)	Cyl. Dia., cm	13.10	12.56		12.6
	Slab Thickness, cm	3.20	2.82		2.8

REFERENCES

1. H. K. Clark. Computer Codes for Nuclear Criticality Safety Calculations. USAEC Report DP-1121, E. I. du Pont de Nemours & Co., Savannah River Laboratory, Aiken,SC (1967).

2. W. W. Engle, Jr. A User's Manual for ANISN. USAEC Report K-1963, Union Carbide Corporation, Nuclear Division, Oak Ridge, TN (1967).

3. L. M. Petrie and N. F. Cross. KENO-IV, An Improved Monte Carlo Criticality Program. USERDA Report ORNL-4938, Oak Ridge National Laboratory, Oak Ridge, TN (1975).

4. H. C. Honeck. The JOSHUA System. USERDA Report DP-1380, E. I. du Pont de Nemours & Co., Savannah River Laboratory, Aiken, SC (1975).

5. H. K. Clark. "Ensuring the Validity of Calculated Subcritical Limits." Trans. Am. Nucl. Soc. 28, 281-282 (1978).

6. G. E. Hansen and W. H. Roach. Six and Sixteen Group Cross Sections for Fast and Intermediate Critical Assemblies. USAEC Report LAMS-2543, Los Alamos Scientific Laboratory, Los Alamos, NM (1961).

7. H. J. Amster. A Compendium of Thermal Neutron Cross Sections Averaged Over the Spectra of Wigner and Wilkins. USAEC Report WAPD-185, Bettis Plant, Pittsburgh, PA (1958).

8. R. C. Lloyd, C. R. Richey, E. D. Clayton, and D. R. Skeen. "Criticality Studies with Plutonium Solutions." Nucl. Sci. Eng. 25, 165-173 (1966).

9. Francis Barbry, Jean-Claude Bouly, Robert Caizergues, Edouard Deilgat, Michel Houelle, Pierre Lecorche. Etude Experimental et Theorique de L'Empoisonnement Heterogen de Solution de Matiere Fissile par des Tubes ou des Anneaux en Verre au Borosilicate. Commissariate A L'Energie Atomique Report CEA-R-3931, Secretariat General du Gouvernement, Direction de la Documentation, Paris, France (1969).

10. R. C. Lloyd, S. R. Bierman, and E. D. Clayton. "Criticality of Plutonium Nitrate Solutions Containing Borated Rashig Rings." Nucl. Sci. Eng. 50, 127-134 (1973).

11. Reactor Handbook, Fuel Reprocessing, Vol. II, p 445, Interscience Publishers, Inc., New York, NY (1961).

12. J. G. Guibergia. Densite' des Solutions Nitriques de Plutonium Commissariat A L'Energie Atomique Report CEA-RA-3931, Secretariat General du Gouvernement, Direction de la Documentation. Paris, France (1960).

13. C. R. Richey. "Theoretical Analyses of Homogeneous Critical Experiments." Nucl. Sci. Eng. 31, 32-39 (1968).

14. C. R. Richey. "Corrigendum." Nucl. Sci. Eng. 49, 246 (1972).

15. J. E. Suich and H. C. Honeck. The HAMMER System. USAEC Report DP-1064, E.I. Du Pont de Nemours & Co., Savannah River Laboratory, Aiken, SC (1967).

16. H. C. Honeck and D. R. Finch. FLANGE II (Version- 71-1). USAEC Report DP-1278, E.I. Du Pont de Nemours & Co., Savannah River Laboratory, Aiken, SC (1971).

17. K. D. Lathrop and B. G. Carlson. Discrete Ordinates Angular Quadrature of the Neutron Transport Equation. USAEC Report LA-3186, Los Alamos Scientific Laboratory, Los Alamos, NM (1965).

18. V. C. Boffi and F. Premuda. "Two-Group Neutron Transport Theory for a Finite Critical Slab." Nucl. Sci. Eng. 38, 205 (1969).

19. H. G. Kaper, A. J. Linderman, and G. K. Leof. "Benchmark Values for the Slab and Sphere Criticality Problem in One-Group Neutron Transport Theory." Nuc. Sci. Eng. 54, 94-99 (1974).

20. R. G. Soltesz et al. Nuclear Rocket Shielding Methods Modification, Updating, and Input Data Preparation, One-Dimensional Discrete Ordinates Transport Technique, Final Progress Report, Vol. IV. Westinghouse Report WANL-PR (LL)-034 (Vol. 4), Westinghouse Astronuclear Laboratory, Pittsburg, PA (1970).

21. Radiation Shielding Information Center newsletter. Oak Ridge National Laboratory, No. 188, August 1980.

22. H. C. Paxton. Experimental Criticality Specifications - An Annotated Bibliography Through 1977. USAEC Report LA-7170-MS, Ann Alamos Scientific Laboratory, Los Alamos, NM (1978).

23. B. M. Durst, S. R. Bierman, and E. D. Clayton. Handbook of Critical Experiments Benchmarks. USERDA Report PNL-2700, Battelle Pacific Northwest Laboratories, Richland, WA (1978).

24. F. E. Kruesi, J. O. Erkman, and D. D. Lanning. Critical Mass Studies of Plutonium Solutions. USAEC and GE Report HW-24514, Hanford Atomic Products Operation, Richland, WA (1952).

25. R. C. Lloyd, R. A. Libby, and E. D. Clayton. "Limiting Critical Concentration and Eta for ^{239}Pu." Trans. Am. Nucl. Soc. 28, 292-293 (1978).

26. R. Gwin and D. W. Magnuson. "The Measurement of Eta and Other Nuclear Properties of ^{233}U and ^{235}U in Critical Aqueous Solutions." Nucl. Sci. Eng. 12, 364-380 (1962).

27. R. C. Lloyd, E. D. Clayton, L. E. Hansen, and S. R. Bierman. "Criticality of Plutonium Nitrate Solutions in Slab Geometry." Nucl. Technol. 18 225-230 (1973).

28. R. C. Lloyd, E. D. Clayton, and L. E. Hansen. "Criticality of Plutonium Nitrate Containing Soluble Gadolinium." Nucl. Sci. Eng. 48, 30304 (1972).

29. R. C. Lloyd and E. D. Clayton. "The Criticality of High Burnup Plutonium." Nucl. Sci. Eng. 52, 73-75 (1973).

30. C. R. Richey, J. D. White, E. D. Clayton, and R. C. Loyd. "Criticality of Homogeneous Plutonium Oxide-Plastic Compacts at H:Pu = 15." Nucl. Sci. Eng. 23, 150-158 (1965).

31. L. E. Hansen, E. D. Clayton, R. C. Lloyd, S. R. Bierman, and R. D. Johnson. "Critical Parameters of Plutonium System - Part I: Analysis of Experiments." Nucl. Appl. 6, 371-380 (1969).

32. S. R. Bierman, L. E. Hansen R. C. Lloyd, and E. D. Clayton. "Critical Experiments with Homogeneous PuO_2 - Polystyrene at 5H/Pu." Nucl. Appl. 6, 23-26 (1969).

33. S. R. Bierman and E. D. Clayton. "Critical Experiments with Unmoderated Plutonium Oxide." Nucl. Technol. 11, 185-190 (1971).

34. S. R. Bierman and E. D. Clayton. "Critical Experiments with Homogenenous PuO_2 - Polystyrene at 50 H/Pu." Nucl. Technol. 15, 5-13 (1972).

35. S. R. Bierman and E. D. Clayton. "Critical Experiments with Low-Moderated Homogeneous Mixture of Plutonium and Uranium Oxides Containing 8, 15, and 30 wt% Plutonium." Nucl. Sci. Eng. 61, 370-376 (1976).

36. G. E. Hansen and H. C. Paxton. Re-Evaluated Critical Specifications of Some Los Alamos Fast-Neutron Systems. USAEC Report LA-4208, Los Alamos Scientific Laboratory, Los Alamos, NM (1969).

37. D. R. Smith and W. U. Geer. "Critical Mass of a Water-Reflected Plutonium Sphere." Nucl. Appl. Technol. 1, 405-408 (1969).

38. H. K. Clark. "Establishing Subcritical Limits." Nuclear Criticality Safety. USAEC Report TID-26286, Technical Information Center, Office of Information Services, Springfield, VA (1974).

39. H. K. Clark. "Bucklings of Pu-H_2O Systems." USAEC Report DP-701, E. I. du Pont de Nemours & Co., Savannah River Laboratory, Aiken, SC (1962).

40. E. D. Clayton et al. "Basis for Subcritical Limits in Proposed Criticality Safety Standard for Mixed Oxides." Nucl. Technol. 35, 97-111 (1977).

41. C. R. Richey. "Theoretical Analyses of Homogenous Critical Experiments." Trans. Am. Nuc. Soc. 9, 515-516 (1966).

42. H. K. Clark. Handbook of Nuclear Safety. USAEC Report DP-532, E. I. du Pont de Nemours & Co., Savannah River Laboratory, (1961).

43. H. K. Clark. "Effect of Distribution of Fissile Material on Critical Mass." Nucl. Sci. Eng. 24, 133-141 (1966).

44. H. C. Paxton, J. T. Thomas, D. Callihan, and E. B. Johnson. Critical Dimensions of Systems Containing U-235, Pu-239, and U-233. USAEC Report TID-7028, Division of Technical Information, Oak Ridge, TN (1964).

45. H. K. Clark. "Minimum Critical Concentration of Pu 239." Trans. Am. Nucl. Soc. 17, 278-279 (1973).

46. C. R. Richey. "Re-examination of the value for the Minimum Critical Concentration of ^{239}Pu in Water." Nucl. Sci. Eng. 55, 244 (1974).

APPENDIX A

Conversion of Resonance Reaction Rates to Cross Sections

The conversion is done as follows. For a group, g, of lethargy width Δu_g containing resonances, the reaction rate is

$$R_{og} = \int_{u_1}^{u_2} \Sigma_a(u)\, \phi(u)\, du$$

It is expressed in GLASS as the rate per unit slowing down density. Therefore, if p represents the fraction of fission neutrons not absorbed in higher energy groups (in resonance or otherwise), the actual rate is

$$R_g = p\, R_{og}$$

The macroscopic resonance integral is defined as the ratio of the reaction rate to the flux, Φ_{og}, as a function of lethargy that would exist if there were no resonance. If source neutrons entering the group are normalized to unity,

$$\Sigma_{rg} \int_{u_1}^{u_2} \phi_{og}\, du = 1,$$

where Σ_{rg} is the removal cross section. Since the flux as a function of lethargy (in the absence of absorption) is flat,

$$\phi_{og} = \frac{1}{\Sigma_{rg}\, \Delta u_g}$$

The macroscopic integral I_g is thus

$$I_g = R_{og}\, \Sigma_{rg}\, \Delta u_g$$

The solution of the slowing down equation in the asymptotic case with constant scattering cross section and no absorption (or leakage) yields

$$\Sigma_{rg} = \frac{\xi \Sigma s}{\Delta u_g}$$

Thus, $I_g = R_{og}\ \xi\Sigma s$.

The presence of the resonance in group g alters the cross section for removal by scattering, but the altered removal matrix is not usually obtained. In any case, it is preferable to use the removal matrix generated in the absence of resonance absorption to permit cross section combinations to be made readily. To maintain the same reaction rate in group g due to resonance absorption, the resonance absorption cross section Σ_{ag} must be such that

$$\Phi_g\ \Sigma_{ag} = R_g$$

where $\Phi_g = \int_{u_1}^{u_2} \phi(u)\ du$. But

$$\Phi_g = \frac{Q_g}{\Sigma_{ag} + \Sigma_{tg} - \Sigma_{gg}}$$

where Σ_{tg} is the total (transport) cross section, including smooth absorption and transfer to other groups in the absence of resonance absorption, where Σ_{gg} is the self scatter cross section under the same conditions, and where Q_g represents neutrons transferred to group g from higher energy groups and any contribution from fission. Eliminating Φ_g and solving for Σ_{ag} yields

$$\Sigma_{ag} = \frac{(\Sigma_{tg} - \Sigma_{gg})}{Q_g - R_g}\ R_g \qquad (1)$$

In the KOKO subroutines, Q_g is determined by solving the slowing down equations with zero leakage and a unit fission source. In each group where resonance absorption occurs, Σ_{ag} is determined and is added to Σ_{tg} and to the smooth absorption cross section to produce multigroup cross sections that contain resonance absorption. Track is kept of absorptions (both smooth and resonance) that occur in order to obtain p, which is required for obtaining R_g from R_{og}.

As has been pointed out above, the flux in the absence of the resonance in group g is

$$\phi_{og} = \frac{Q_g}{\Sigma_{rg}\ \Delta u_g}$$

where $\Sigma_{rg} = \Sigma_{tg} - \Sigma_{gg}$. This flux contains allowance for absorption in higher energy groups; hence, the macroscopic resonance integral is

$$I_g = \frac{R_g}{\phi_{og}}$$

Thus,

$$\frac{I_g}{\Delta u_g} = \frac{R_g \Sigma_{rg}}{Q_g} \tag{2}$$

Using (2) to eliminate Qg from (1) yields

$$\Sigma_{ag} = \frac{I_g/\Delta u_g}{1 - \frac{I_g/\Delta u_g}{\Sigma_{rg}}} \tag{3}$$

This formula presumes an accurate calculation of the resonance integral or alternatively of the resonance reaction rate. Too large a resonance integral, especially for highly undermoderated systems, can lead to negative cross sections as was found to be the case for ^{233}U in UH_3 whether the cross sections were drawn from the Standard or the ENDF/B-IV library. To prevent negative cross sections in cases where Rg exceeds Qg, Rg is arbitrarily set equal to 0.99 Qg.

The term in the denominator of (3) or equivalently of (1) appears frequently to be omitted. Thus, Nordheim (Theory of Resonance Absorption - Proceedings of Symposia in Applied Mathematics, Volume XI 1961, page 61) gives

$$\Sigma_{ag} = \frac{\Sigma I_i}{\Delta u_g}$$

where the sum is taken over the resonance integrals within the group. Similarly, the term in the denominator is not used in conjuction with Hansen-Roach cross sections. Although inclusion of the term is certainly correct if the resonance integral or reaction rate is calculated accurately, omitting it may tend to compensate for approximations commonly made in computing the resonance integral. If resonance absorption within a group is small, it makes little difference, of course, whether or not it is included.

APPENDIX B

Example of Minimum Critical Parameter Derivation

The minimum critical mass for $^{239}Pu(NO_3)_4$ was calculated by HRXN-ANISN by: 1) selecting concentrations over the range within which the minimum is expected to lie, 2) computing the values of $H/^{239}Pu$ and reading the critical values of k_{eff} from Figure 1, and 3) computing the masses of water-reflected spheres at these values of k_{eff} as indicated in Table B-1. The masses were then plotted against concentration as in Figure B-1 and the minimum value was thereby determined.

TABLE B-1

Determination of Minimum Critical Mass of ^{239}Pu as $Pu(NO_3)_4$

Conc of Pu, M/L	*Conc of NO_3, M/L*	*$H/^{239}Pu$*	*Critical k_{eff}*	*Mass@ Critical k_{eff}, g*
0.1	0.40	1100	1.0006	565.8
0.12	0.48	915.2	0.9966	539.0
0.14	0.56	783.2	0.9948	537.4
0.16	0.64	684.2	0.9937	547.1
0.18	0.72	607.1	0.9932	563.7

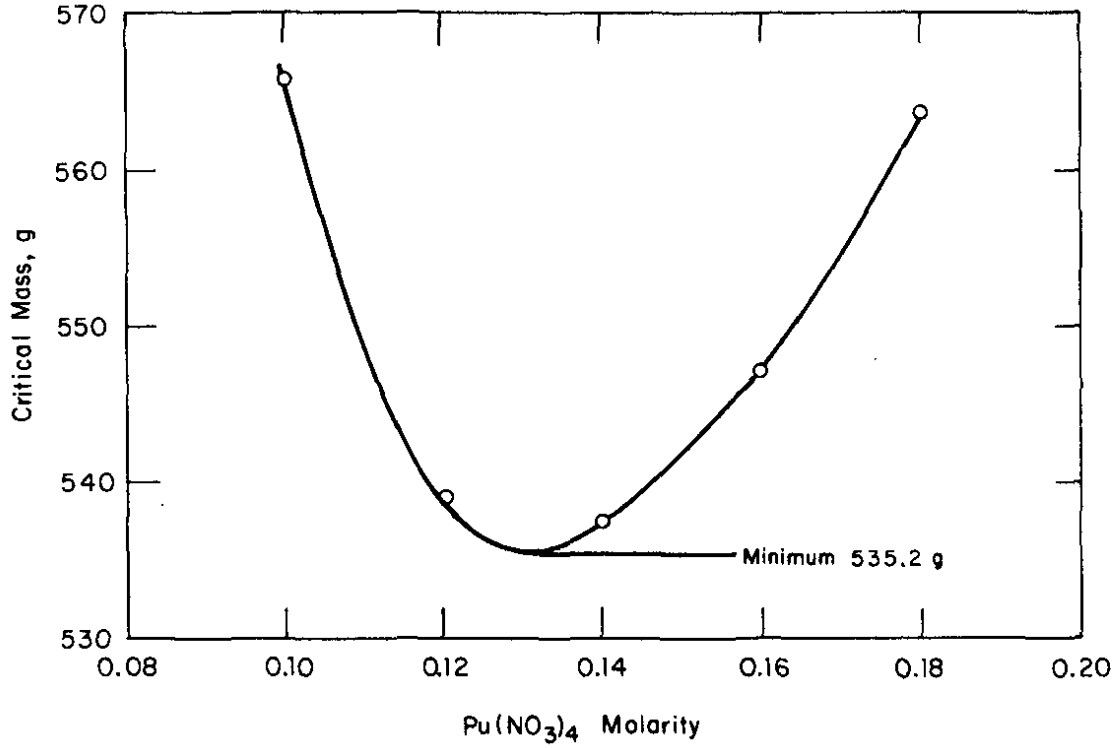

FIGURE B-1. Determination of Minimum Critical Mass of ^{239}Pu